2016

A 2X2 Polarization Switchable Patch Antenna Array For Polarization Modulation

Pengfei Ji
Minnesota State University Mankato

A 2X2 Polarization Switchable Patch Antenna Array For Polarization Modulation

By

Pengfei Ji

A Thesis Submitted in Partial Fulfillment of the

Requirements for the Degree of

MASTER OF SCIENCE

In

Electrical and Computer Engineering & Technology

Minnesota State University, Mankato

Mankato, Minnesota

May 2016

April 7 2016

A 2X2 Polarization Switch Patch Antenna Array For Polarization Modulation

Pengfei Ji

This thesis has been examined and approved by the following members of the student's committee.

Xuanhui Wu_____
Advisor

Qun Zhang_____
Committee Member

Han-Way Huang_____
Committee Member

Abstract

This thesis introduced and investigated a new concept in the development of a 2X2 polarization switchable patch antenna array for polarization modulation. Polarization modulation is a technique to modulate digital information using different polarization of the electromagnetic wave. The existing waveform based modulation techniques are well developed and start approaching to their performance limits. Polarization modulation provides a new modulation dimension for wireless communications and can further increase data throughput. A four-port circular patch antenna is presented and investigated for the implementation of polarization modulation. It has four ports, each excites radiation of a different polarization. A single pole four throw RF switch is used to switch between the ports depending on the information symbol to be transmitted. Then, the antenna is transformed to a 2X2 antenna array to increase the directivity and gain. The antenna is studied numerically and it shows good performance.

Keywords— Patch Antenna, Polarization Modulation, Wireless Communications, 2X2 Antenna Array

Acknowledgments

First of all, I would like to thank my wife, Yun Li, for all her love and support through my studies. Our four years of marriage have been the most joyous experience in my life.

I would especially like to thank my advisor, Dr. Xuanhui Wu, for introducing me to the wonders of antenna research. I thank him for his continuous patience guidance, encouragement and support during the development of this work. He always taught me all the knowledge about RF Engineering, and provided the fundamental thoughts for this research. Without his guidance, I would have never been able to complete this work.

I would also like to thank my committee members, Dr. Qun Zhang and Dr. Han-Way Huang for their encouragement and support in my Graduate studies.

In addition, thanks to my fellow classmates, Danyang Huang and Zhewei Gu, for their kindness help in HFSS and HyperLynx 3D softwares.

Finally, I would like to thank my family for their support and understanding that I had to leave my hometown in China to pursue this work.

LIST OF CONTENTS

LIST OF TABLES

LIST OF FIGURES

Chapter 1 Introduction

In recent years, microstrip or patch antennas are becoming increasingly useful because it can be constructed using printed circuit fabrication techniques such that a portion of the metallization layer is responsible for radiation. The benefits of patch antennas are easily fabricated and low cost.

In digital communications, discrete data symbols are modulated using the amplitude, frequency or phase of a waveform. Such waveform based modulation schemes are well developed and start approaching their performance limits with the use of advanced channel coding and signal processing. To further increase channel capacity, additional modulation dimensions should be sought. Polarization modulation [1] provides an additional degree of freedom to modulate information. Specifically, different data symbols can be represented using identical waveforms but with different polarizations. Thus, bit rate can be increased without additional bandwidth or transmission power. For point-to-point wireless communications [2], where the light-of-sight signal component dominates the received signal, the wave polarization is stable in the channel. So, the polarization modulation technique could be used for point-to-point wireless communications. Polarization reconfigurable antenna [3] could be used to transmit and receive polarization switchable radiation.

To implement the polarization modulation scheme, we design an antenna that is able to transmit waves of different polarizations. Herein, a circular patch antenna [4] with four

ports, each excites a unique linear polarization, is proposed. A single pole four throw RF switch is used to activate one of the four ports. The antenna is studied numerically using HyperLynx 3D EM. Its characteristics such as impedance matching and radiation patterns are investigated.

Chapter 2 Fundamental Theory

2.1 Microstrip Patch Antenna

Microstrip patch antenna usually can be fabricated on printed circuit board. A microstrip device has very simplest form. The device have two conductor structure layers, and those two conductor layers are separated by a thin dielectric substrate. The upper conductor layer consist of a microstrip transmission line which is a long narrow metallization strip and a patch. The lower conductor structure layer is acting as a ground plane.

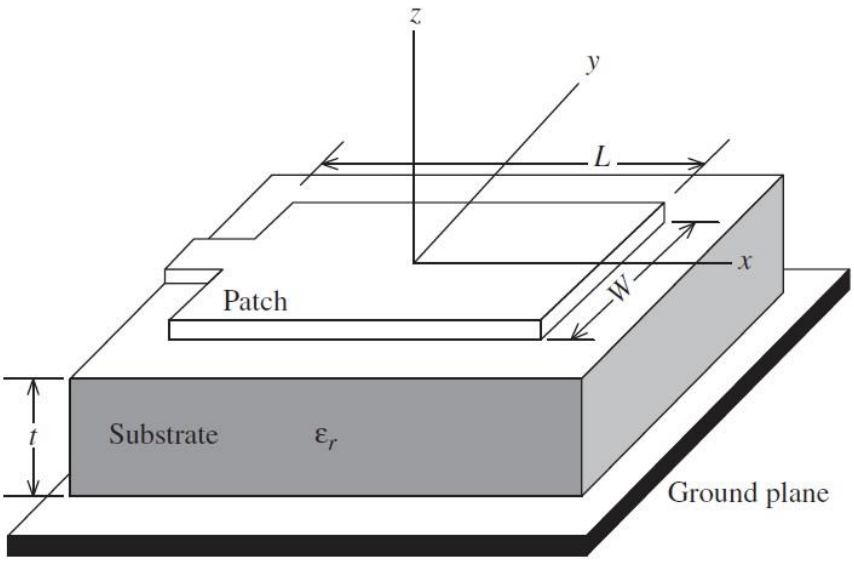

Fig. 1 Geometry of the edge-fed microstrip patch antenna [5]

2.1.1 Half-wavelength rectangular microstrip patch antennas

As the Fig.1 shown, the most common patch antenna is rectangular patch antenna, and the patch is fed by microstrip transmission line. The patch antenna, microstrip

transmission line and ground plane are made of high conductivity metal, which typically use copper. The size of the patch is of length L, width W, and sitting on top of a dielectric circuit board of thickness t with permittivityε_r. The edge feed is a microstrip transmission line on the left side of the patch [5]. The thickness of substrate is considered important when we design microstrip patch antennas. For antennas preformance, the thick with a low dielectric constant substrate will be chosen to design microstrip patch antennas [6].

The fringing fields act to extend the effective length of the patch, so the length of a half-wave patch is slightly less than a half wavelength in the dielectric substrate meterial. The frequency of operation of the patch antenna is determined by the length L [7]. The value of the center frequency will be approximately given by:

$$f_c \approx \frac{c}{2 \times L \times \sqrt{\varepsilon_r}} = \frac{1}{2 \times L \times \sqrt{\varepsilon_0 \varepsilon_r \mu_0}}$$

If the center frequency is known, we could calculate the approximate value of the length of a resonant half-wavelength patch by:

$$L \approx \frac{c}{2 \times f_c \times \sqrt{\varepsilon_r}} = \frac{\lambda}{2 \times \sqrt{\varepsilon_r}} \approx 0.49 \times \lambda_d$$

Where $\varepsilon_r$is the substrate dielectric constant, λ the free space wavelength, λ_d the wavelength in the dielectric.

2.1.2 Radiation Pattern

One of the very important parameter in antennas design is radiation pattern. Antenna radiation pattern is defined as a mathematical function or a graphical method to depict the field strength transmitted from or received by the antenna. Antenna radiation patterns are usually shown in one plane cut, one frequency and one polarization. The patterns are usually presented with a dB strength scale [8].

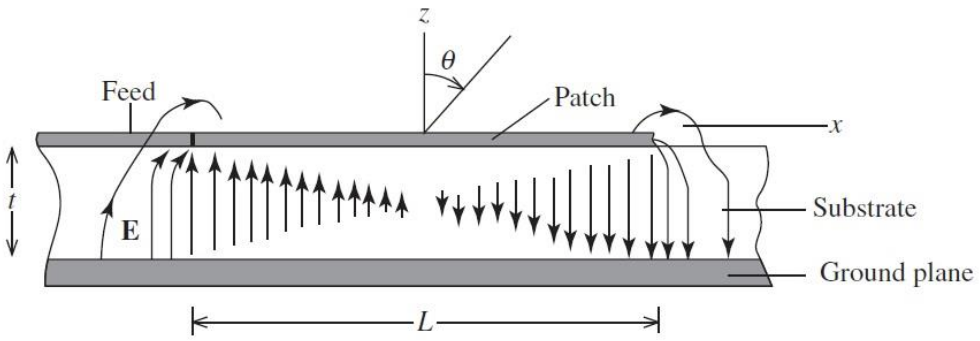

Fig. 2 Side View of Patch Antenna [5]

The Fig.2 shows side view of patch antenna. The electric field of standing wave mode is very clearly shown in the dielectric circuit board. The signal is excited from the feeding transmission line to the patch, so the electric field is required to perpendicular from patch to ground by boundary conditions [9]. The electric field at broadside of dielectric circuit board is opposite phase on the left and right halves because the standing wave mode with a half-wavelength is separated between the ends. The total fringing field is 180^{o} out of phase and same magnitude at broadside, so their radiation will be canceled [10].

As Fig.3 shown, the fringing electric fields on the edge of the microstrip patch add up in phase and product radiation of the microstrip patch antenna [11]. The peak radiation pattern is in the $+z$ direction.

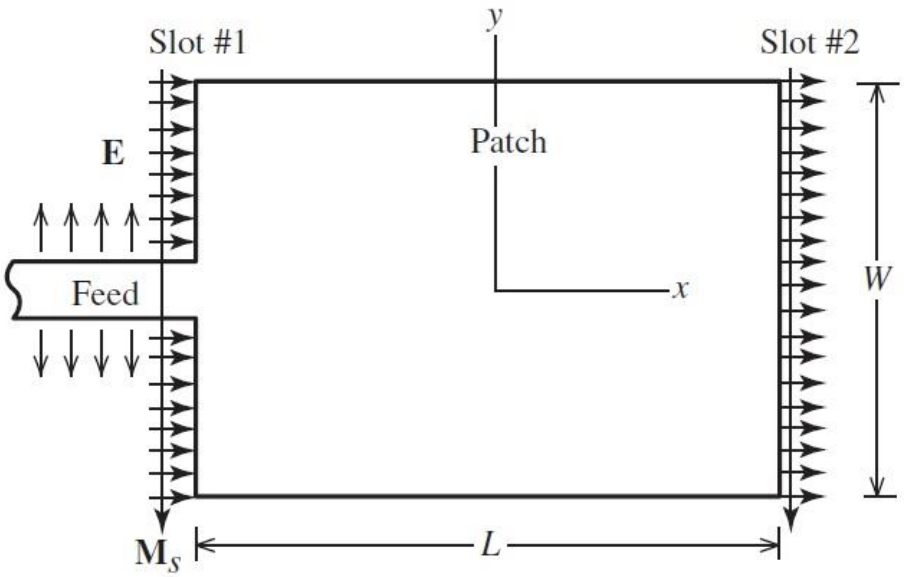

Fig. 3 Top View of Patch Antenna [5]

The equivalent magnetic surface currents density is along the edge of the microstrip patch [12]. Base on the image theory to account for the ground plane, the equation is given by:

$$\overrightarrow{M_s} = -2\hat{n} \times \overrightarrow{E_a}$$

Where the $\overrightarrow{E_a}$ is the fringing electric field in each of the edge slots [12]. The normalized radiation pattern is approximately given by:

$$E_\theta = \frac{\sin\left(\frac{kW \sin\theta \sin\varphi}{2}\right)}{\frac{kW \sin\theta \sin\varphi}{2}} \cos\left(\frac{kL}{2} \sin\theta \cos\varphi\right)$$

$$E_\varphi = -\frac{\sin\left(\frac{kW \sin\theta \sin\varphi}{2}\right)}{\frac{kW \sin\theta \sin\varphi}{2}} \cos\left(\frac{kL}{2} \sin\theta \cos\varphi\right) \cos\theta \sin\varphi$$

Where k is the free-space phase constant, $k = 2\pi/\lambda$. The magnitude of the fields is given by:

$$f(\theta, \varphi) = \sqrt{{E_\theta}^2 + {E_\varphi}^2}$$

From above equation, there are two factor to control the radiation pattern. The fist factor is the width W in y-axis of the microstrip patch antenna. The second factor is array factor L. The normalized array for two elements with the same magnitude and phase is separated by the distance L in x-axis [13].

2.1.3 Microstrip Transmission Line

The microstrip transmission line is shown in Fig.4 as the feeding line. The microstrip transmission line is also can be fabricated by using printed circuit board technology. It consists of a conducting metal strip and a ground plane. The conducting strip and ground plane are separated by a dielectric layer known as the substrate [14]. The advantages of microstrip transmission line are easily fabricated and low cost;

however, the disadvantages are the generally lower power handing capacity and higher losses.

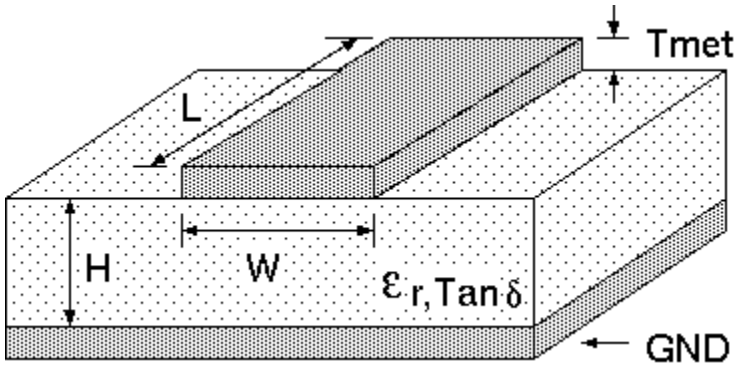

Fig. 4 Geometry of Microstrip Transmission Line

Reflection coefficient is the other very important parameter for microstrip transmission line known as S11 parameter. This parameter is describes how much of an electromagnetic wave is reflected by an impedance mismatching in the transmission line [15]. As Fig.5 shown, a microstrip transmission line with impedance Z_0 terminated in a load impedance Z_L.

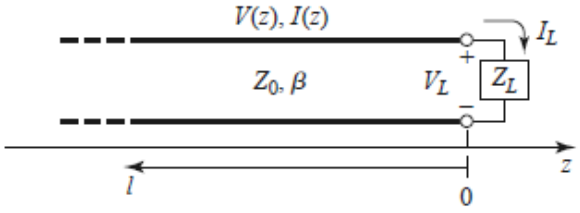

Fig. 5 A Transmission Line with a load impedance Z_L

The incident voltage wave generated from a source to transmission line can be formed as $V_0^+ e^{-j\beta z}$ $(Z < 0)$. The reflected voltage wave from the load impedance to transmission line can be formed as $V_0^- e^{j\beta z}$. The total voltage wave on the transmission line can be written by

$$V(z) = V_0^+ e^{-j\beta z} + V_0^- e^{j\beta z}$$

The total current wave on the transmission line can be described by

$$I(z) = \frac{V_0^+}{Z_0} e^{-j\beta z} - \frac{V_0^-}{Z_0} e^{j\beta z}$$

At Z=0, we can use the total voltage and total current to calculate the load impedance.

$$Z_L = \frac{V(0)}{I(0)} = \frac{V_0^+ + V_0^-}{V_0^+ + V_0^-} Z_0$$

Then, solving the V_0^- by

$$V_0^- = \frac{Z_L - Z_0}{Z_L + Z_0} V_0^+$$

So, the voltage reflection coefficient is defined as the ratio of reflected voltage wave to the incident voltage wave. The reflection coefficient is usually described as dB.

$$\Gamma = \frac{V_0^-}{V_0^+} = \frac{Z_L - Z_0}{Z_L + Z_0}$$

From this equation, we should know when Z_L is equal to Z_0, the reflection coefficient Γ should be zero in this microstrip transmission line [16]. That means the impedance of transmission line is matching the impedance of the load, and the maximum power

is delivered to the load. When Γ is not equal to zero, the load is mismatched to microstrip transmission line. That means some of the power from the source is reflected by the load as known Return Loss (RL).

$$RL = -20log|\Gamma|\ dB$$

Note that the value of reflection coefficient is usually negative, but the value of return loss is nonnegative.

Base on the Ohm's law, we can calculate the impedance by using the incident voltage wave and current generated from a source to transmission line [].

$$V^+ = E \cdot h \qquad I^+ = Js \cdot W = H \cdot W$$

$$Z_0 = \frac{V^+}{I^+} = \frac{E \cdot h}{H \cdot W} = \sqrt{\frac{\mu}{\varepsilon}} \cdot \frac{h}{W}$$

Where E is the total E field, h is the thickness of the dielectric substrate, H is the total magnetic field, and W is the width of the microstrip transmission line [17]. From the equation, we can determine that the thickness of the dielectric substrate and the width of the microstrip transmission line are the critical factor to control the impedance of microstrip transmission line.

When we design a new microstrip transmission line Z_M to insert between the generator transmission line and the load, the matching impedance is desired to be Z_0 for this transmission line. If the length of the transmission line is $z = -l$ from the load, the input impedance toward the load is

$$Z_{in} = \frac{V(-l)}{I(-l)} = \frac{V_M^+(e^{j\beta l} + \Gamma e^{-j\beta l})}{V_M^+(e^{j\beta l} - \Gamma e^{-j\beta l})} Z_M = \frac{e^{j\beta l} + \Gamma e^{-j\beta l}}{e^{j\beta l} - \Gamma e^{-j\beta l}} Z_M$$

We also know the reflection coefficient equation, so the input impedance will be

$$Z_{in} = \frac{(Z_L + Z_M)e^{j\beta l} + (Z_L - Z_M)e^{-j\beta l}}{(Z_L + Z_M)e^{j\beta l} - (Z_L - Z_M)e^{-j\beta l}} Z_M = \frac{Z_L + jZ_M \tan \beta l}{Z_M + jZ_L \tan \beta l} Z_M = Z_0$$

Where the $\beta = \frac{2\pi}{\lambda_g}$, so when $l = \frac{\lambda_g}{4}$, $\beta l = \frac{\pi}{2}$ then $\tan \beta l = +\infty$. The input impedance will be

$$Z_{in} = \frac{Z_M}{Z_L} Z_M = Z_0 \ \rightarrow \ Z_M = \sqrt{Z_L \cdot Z_0}$$

If the length of the new transmission line is quarter wavelength, the impedance of the new transmission line should be the $\sqrt{Z_L \cdot Z_0}$. If the length is half wavelength, the impedance of the new transmission line will be same as Z_0.

2.2 Polarization Modulation

In digital communication and antenna design, modulation is usually used as a process of converting the modulating signal with properties of a periodic waveform, called the carrier signal, to be transmitted. There are three basic types of modulation: amplitude modulation, frequency modulation, and phase modulation. In amplitude modulation, the amplitude of carrier signal is used to vary the modulating signal being transmitted [18]. For frequency modulation, the frequency of the carrier signal is varied to be transmitted. For the phase modulation, the phase of the carrier signal is varied to be transmitted.

In phase modulation, binary phase shift keying (BPSK) modulation and quadrature phase shift keying (QPSK) modulation are two important techniques to modulate the

information signal by changing the phase of carrier wave. The data input is digital, and the output is modulated analog spectrum.

2.2.1 Binary Phase Shift Keying (BPSK) Modulation

In BPSK, binary 1 and binary 0 are represented by different carrier phase. The phase of each binary is 180˚ apart as Fig. 6 shown. The two different phases represent the two binary digits [19].

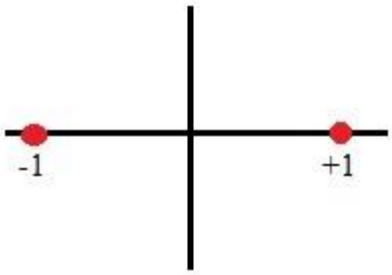

Fig. 6 Binary Phase Shift Keying (BPSK) Constellation diagram

As the Fig.7 shown the BPSK modulation waveform, if the binary 1 is transmitted, the result should be $S(t) = A \cdot \cos(2\pi f_c t)$. If the binary 0 is transmitted, the result should be $S(t) = A \cdot \cos(2\pi f_c t + \pi)$.

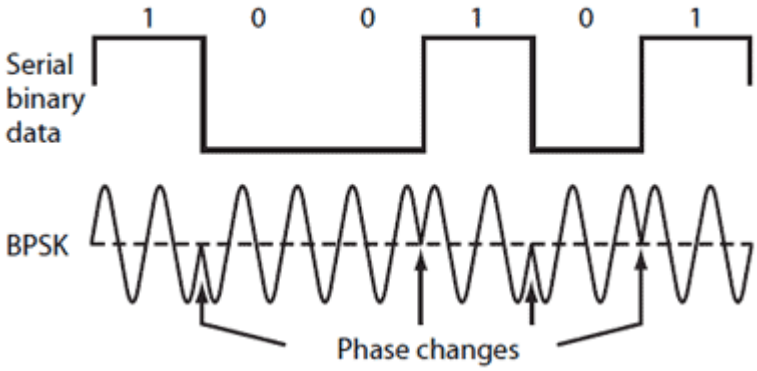

Fig. 7 the BPSK Modulation Waveform [20]

2.2.2 Quadrature Phase Shift Keying (QPSK) Modulation

Compare to BPSK, the QPSK modulation can increase the data rate in the same bandwidth of the signal. QPSK modulation can use four points on the constellation diagram as Fig.8 shown, and each signal point represents two bits.

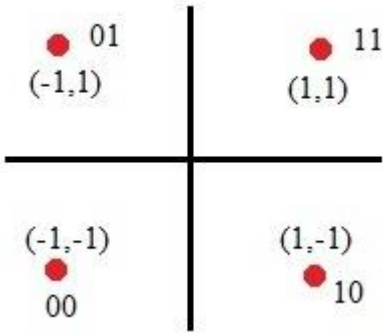

Fig. 8 Quadrature Phase Shift Keying (BPSK) Constellation diagram

As we known, QPSK can encode two bit per symbol by using complex carrier symbol. Each carrier symbol have phase shift by 90˚ apart [21]. The mathematic equation of the QPSK modulation is given in Table.1

Input 1	Input 2	output	Phase shift
0	0	$-1-1*j$	$S(t)=A\cdot\cos\left(2\pi f_c t-\frac{3\pi}{4}\right)$
0	1	$-1+1*j$	$S(t)=A\cdot\cos\left(2\pi f_c t+\frac{3\pi}{4}\right)$
1	0	$1-1*j$	$S(t)=A\cdot\cos\left(2\pi f_c t-\frac{\pi}{4}\right)$
1	1	$1+1*j$	$S(t)=A\cdot\cos\left(2\pi f_c t+\frac{\pi}{4}\right)$

Table. 1 the Input and Output in QPSK Modulation

In QPSK modulation process, the input bit stream has to be separated to two-two bits, then these two bits are sent simultaneously to the input of the QPSK modulator. The output should be the complex data, and each output data has 90˚ phase shift.

2.2.3 Polarization Modulation

Polarization modulation is the critical technique for this research design. The BPSK modulation and QPSK modulation are using scaler waveforms to modulate the data stream. RF or digital circuits by themselves cannot handle vector waveform polarization because a circuit only sense voltage or current which are scalars not vectors. Compare to the BPSK modulation and QPSK modulation, polarization modulation is a new technique to modulate the digital information using different polarization of the electromagnetic wave. As we known, electric field from antenna is a vector, so in this research, we need design an antennas to transmit and sense electric field with different direction. The Fig.9 is shown the polarization modulation constellation diagram, and the arrow is to show the direction of electric field [22].

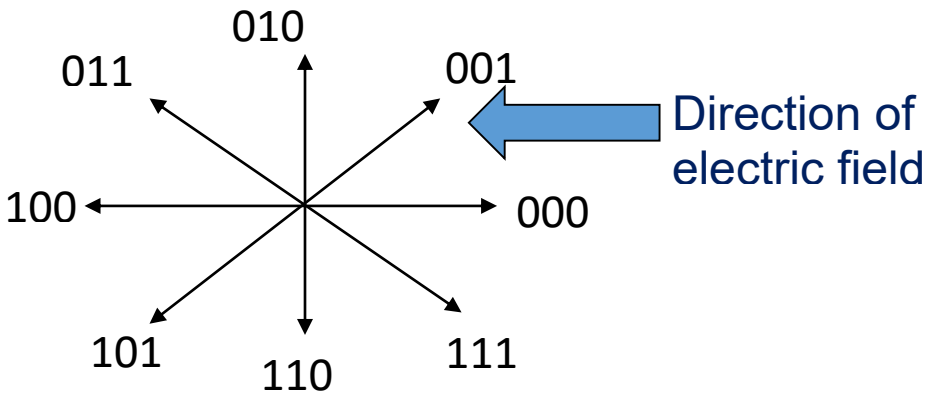

Fig. 9 Polarization Modulation Constellation Diagram

With addition dimension of electric field, the bit rate can be increased in polarization modulation process. The different symbols can be represent using the same waveforms but different polarization direction without increased bandwidth and transmission power [23]. A circular patch antenna with four ports can be used to implement polarization modulation. There are four microstrip lines that feed the antenna. Each of four microstrip lines is excited different linearly polarized fields. The other ends of all the four feeding lines are connected to a single pole four throw RF switch. The control lines of the switch determine only one of the four feeding lines is connected to the RF input.

2.3 Antenna Array

Antenna array theory is introduced to develop the performance of this antenna [25]. The advantage of microstrip antennas array is that the radiating elements can be easily fabricated on a single layer printed circuit board. Sometimes, the single element of patch antenna could not perform very well in directivity and gain, so the 2X2 patch antenna array is designed to improve the gain of this antenna. As the following equation shown,

$$G = \varepsilon_{ap}\frac{4\pi}{\lambda^2}A_P = \varepsilon_{ap}\frac{4\pi}{\lambda^2}L_xL_y = \varepsilon_{ap}\frac{4\pi}{\lambda^2}\left(\sqrt{N}d\right)\left(\sqrt{N}d\right) = \varepsilon_{ap}\frac{4\pi}{\lambda^2}Nd^2$$

Where N is the number of antenna elements, and d is the space of two antenna array elements [26]. When the number of antenna elements and the space are increasing, the gain of the patch antenna array will be improved.

Chapter 3 Antenna Design Process

In this chapter, we will discuss the antenna design process. First of all, we should decide the patch antenna material. Rogers RO4003C printed circuit board is chosen to design this 2X2 polarization switchable patch antenna array because this material offers the high frequency performance and low cost circuit fabrication. The dielectric constant ε_r of Rogers RO4003C is 3.55, and the thickness is 1.524mm. Then, the antenna is constructed by driven patch and parasitic patch. Rogers RO4003C is chosen for both the driven and parasitic boards, which are separated with a spacing of 7mm [26]. The driven patch is printed on the top surface of the driven board and the parasitic patch is printed on the bottom surface of the parasitic board. Finally, the goal of this antenna design is to perform radiation direction in +Z direction, and the reflection coefficient of each part should be less than -14dB between 2.85GHz to 3.15GHz frequency.

3.1 HyperLynx 3D EM Software

For this design, we will choose the HyperLynx 3D EM software (IE3D) to simulate and optimize the 2X2 polarization switchable patch antenna array. This software is an integrated full-wave electromagnetic simulation and optimization package for the analysis and design of 3D and planar microwave circuits, MMIC, RFIC, RFID, antennas, digital circuits and high-speed printed circuit boards (PCB) [27].

First of all, we need to setup the basic parameters of this patch antenna in IE3D. The meshing frequency is 3.15GHz, and the cells per wavelength is 20. Then, we need to create the layers to construct the driven patch and parasitic patch.

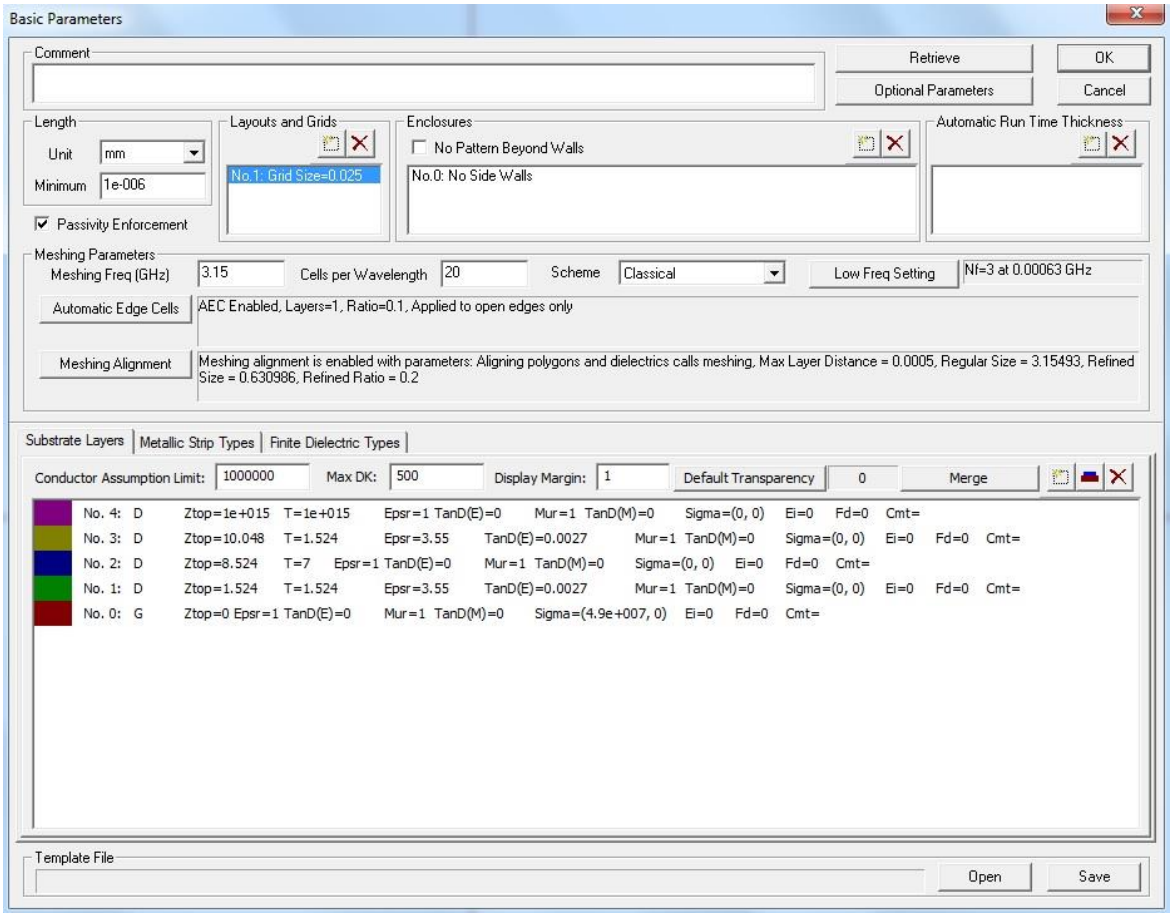

Fig. 10 Basic Parameters setup in IE3D

As Fig.10 shown, layer No.0 is the ground plane. Layer No.1 is the top plane of the driven patch. The distance between layer No.0 and layer No.1 is 1.524mm, which is the thickness of the Rogers RO4003C. The dielectric constant is 3.55. So layer No.0 and layer No.1 construct the driven patch. Layer No.2 is the airgap between the driven patch and

parasitic patch with the thickness of 7mm. Layer No.3 is the bottom plane of the parasitic patch with the thickness of 1.524mm and the dielectric constant of 3.55. Layer No. 4 is the free space plane. So layer No.3 and layer No.4 construct the parasitic patch.

3.2 Patch Antenna with Single Straight Transmission Line

3.2.1 Microstrip Transmission Line Design

In this process, we need start to design a microstrip transmission line. As we known in microstrip transmission line theory, the impedance of most RF device is 50Ω. For the impedance matching, we have to design a transmission line with impedance of 50Ω.

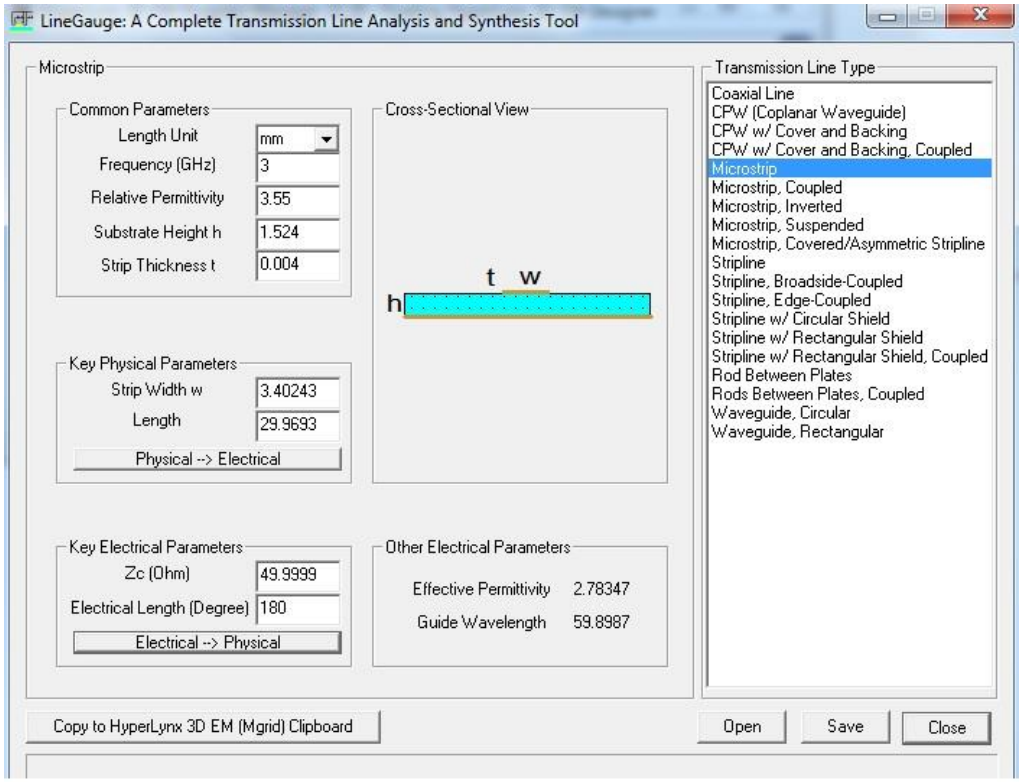

Fig. 11 Microstrip Transmission Line Calculation in IE3D

As the Fig.11 shown, we could use IE3D software to calculate the length and width of the microstrip transmission line. From the datasheets of Rogers RO4003C, we know that the dielectric constant is 3.55, and the thickness of the board is 1.524mm. The impedance of the transmission line should be 50Ω in most RF device. The electrical length should be 180˚ because the impedance is repeated in half wavelength transmission line [28]. After the IE3D calculated, we get the length of the transmission line is 29.9693mm, and the width is 3.40243mm.

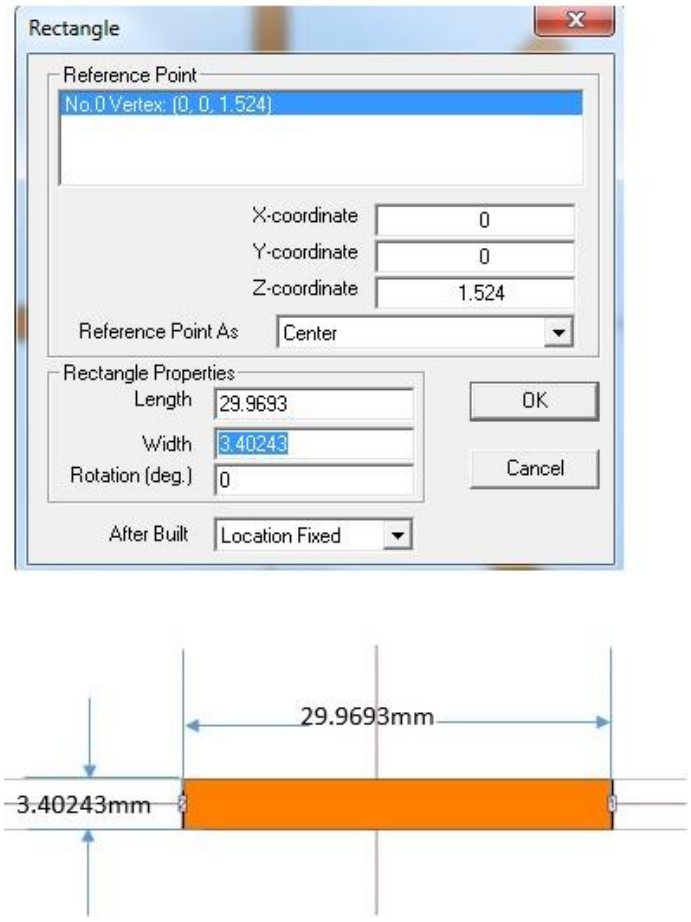

Fig. 12 Geometry of Microstrip Transmission Line

Then, the two ports should be added at the ends of the transmission line. Then, we construct the transmission line as Fig.12 shown. To setup the frequency parameter, we choose 21 frequency points between 2.85GHz to 3.15GHz to simulate and optimize the microstrip transmission line. The goal of reflection coefficient should be less than -40dB. After optimization, the length is changed to 29mm, and width is changed to 3.49mm. The simulation result is shown in Fig.13.

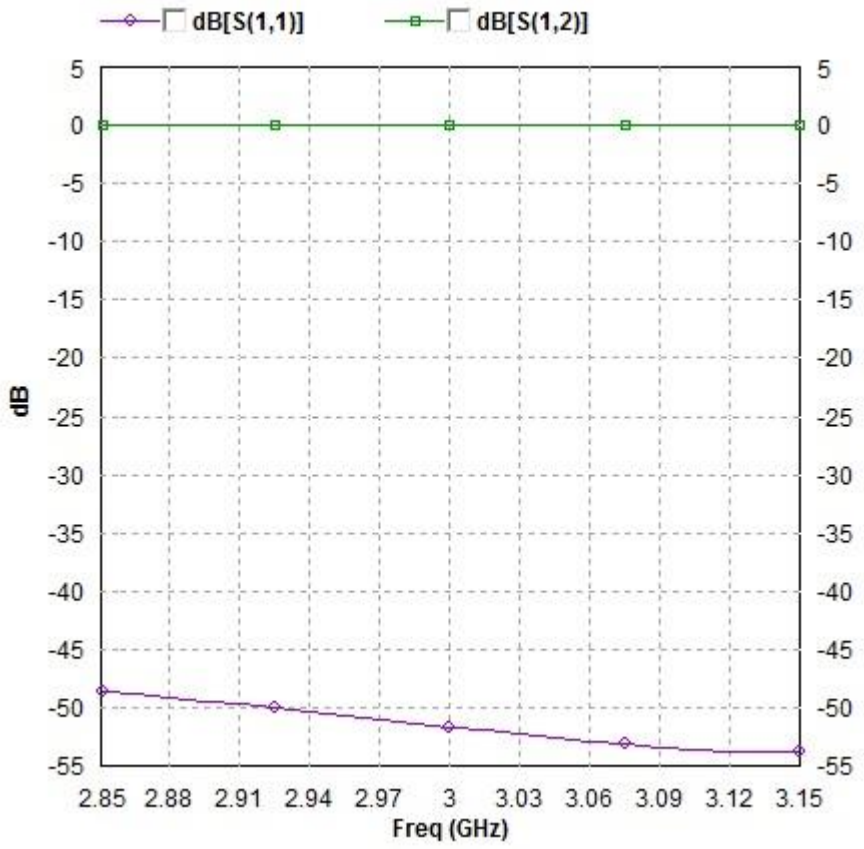

Fig. 13 Reflection Coefficient of Transmission Line

The signal is fed at port1, and out at port2. The reflection coefficient S11 represents how much energy is reflected back at port1. The reflection coefficient S12 represents how much energy is transmitted in transmission line. The result of S11 is less than -47dB, and S12 is close to 0dB. That means most energy will be transmitted in transmission line, and return loss is very small. The result approaches to the goal.

3.2.2 Patch Antenna Design

The single element patch antenna consists of driven patch and parasitic patch. The distant between both patches is 7mm. Base on the microstrip patch antenna theory, the radius of both patches could be approximately calculated. The radius of driven patch is mm, and the radius of parasitic patch is mm.

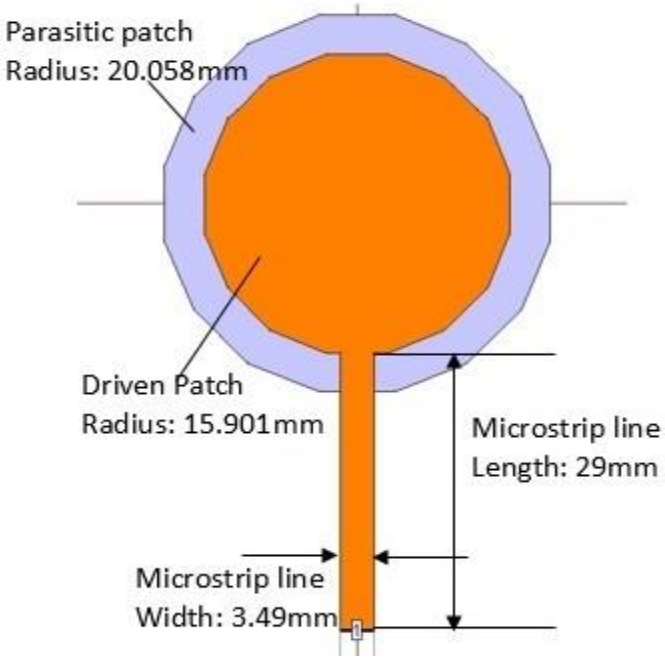

Fig. 14 Geometry of Patch Antenna with Transmission Line

The port is added to the end of transmission line. Then, we keep the values of transmission line, and optimize the radius of both driven patch and parasitic patch. After optimization, the radius of driven patch is changed to 15.901mm, and the parasitic patch is changed to 20.058mm as Fig.14 shown.

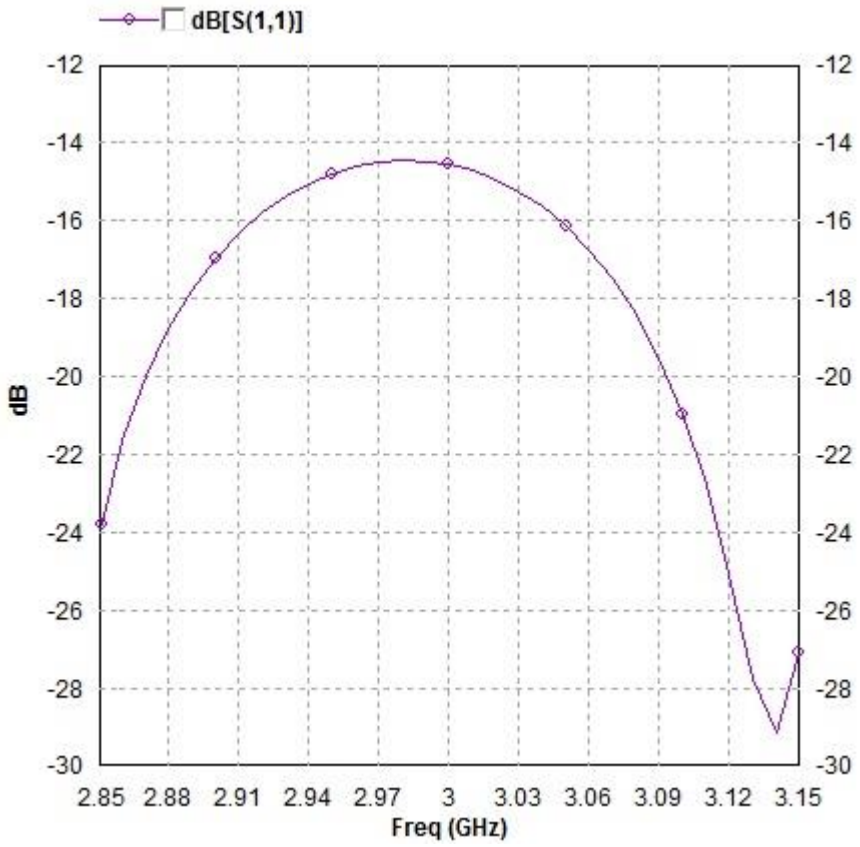

Fig. 15 S11 of Patch Antenna with Transmission Line

The simulation result is shown in Fig.15. The reflection coefficient S11 is less than -11dB which is satisfy to the goal.

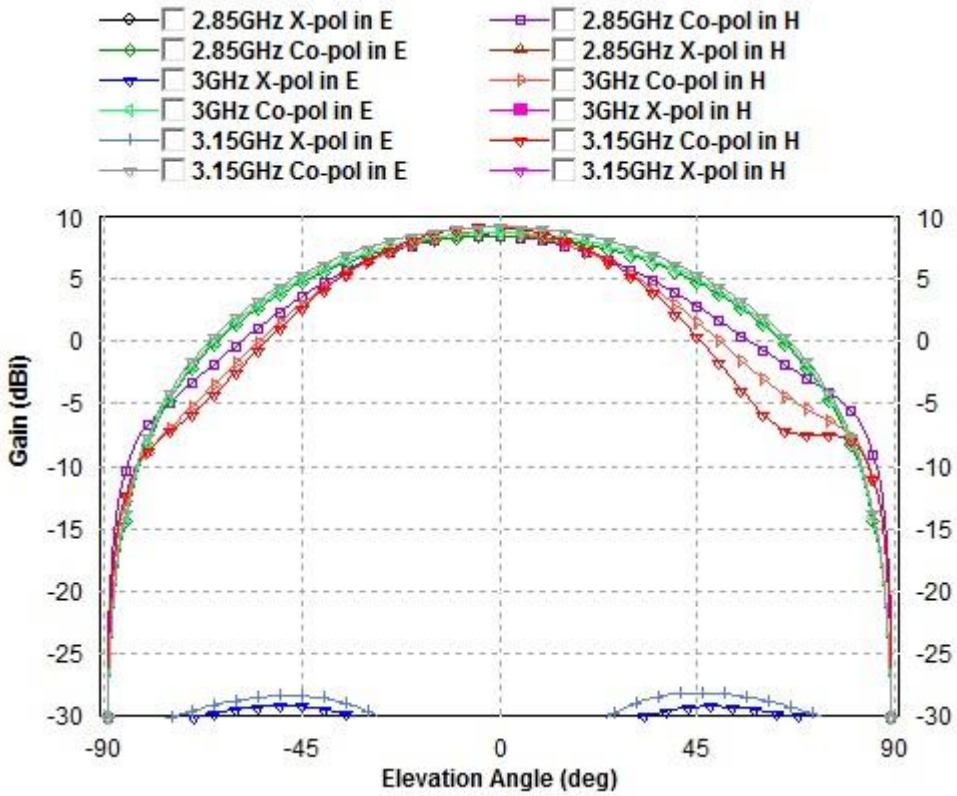

Fig. 16 Radiation Pattern of Patch Antenna with Transmission Line

The result of radiation pattern of single element patch antenna with transmission line is shown in Fig.16. The three frequency observation point are chosen at 2.85GHz, 3GHz and 3.15GHz. It can be seen that the gain value of the cross-pol discrimination in the broadside direction is around 36dB. Clearly, the propagation direction is in +z.

3.3 Patch Antenna with Four Straight Transmission Lines

As we know the polarization modulation theory, this antennas is designed with four microstrip transmission lines that feed the driven patch and excite different linearly polarized fields. Specifically, the Port 1 to Port 4 will generate electric field in vertical

direction, horizontal direction and ±45˚ with the y axis, respectively. The Fig.17 is shown the geometry of single element patch antenna with four transmission lines.

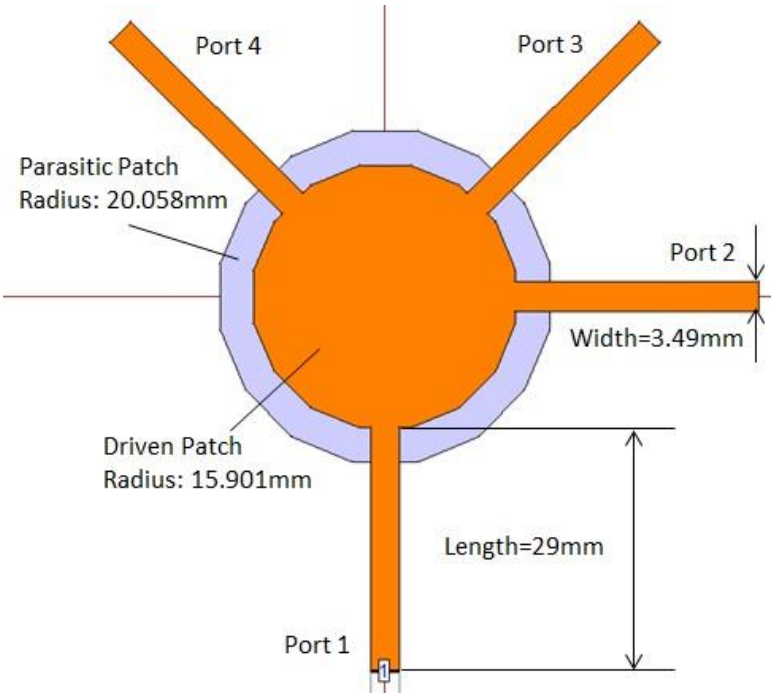

Fig. 17 Geometry of Patch Antenna with Four Straight Transmission Lines

The length of each transmission line is half wavelength as 29mm. This guarantees that each inactive feeding line gives an open circuit at the edge of the driven patch, which produces minimum effects on both the return loss and the radiation characteristics for the excited port. The width of each transmission line is 3.49mm. Then, we excite the port1, and make the other three ports as open circuit to simulate this single element patch antenna.

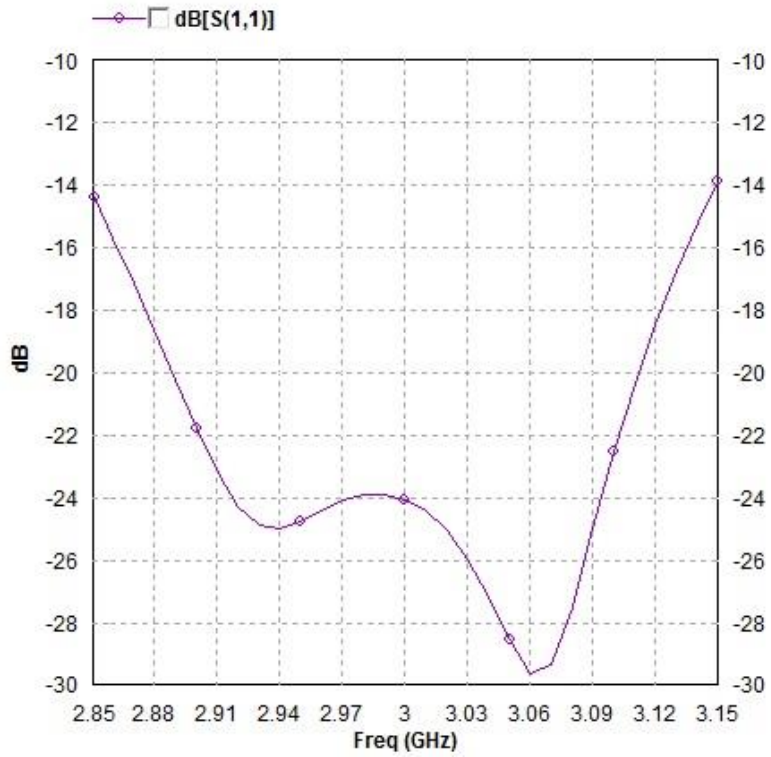

Fig. 18 S11 of Patch Antenna with Four Transmission Lines

The result of reflection coefficient for excited port 1 is shown as Fig.18. From this figure, the S11 parameter is less than -14dB in the frequency between 2.85GHz and 3.15GHz. The S11 result for other three ports is similar to the port1. The result is satisfy to the goal.

The radiation pattern result of excited port1 is shown in Fig.19. At the three frequency observation point 2.85GHz, 3GHz and 3.15GHz, the cross-pol discrimination in the broadside direction is around 22dB. The most energy is radiated in +z direction.

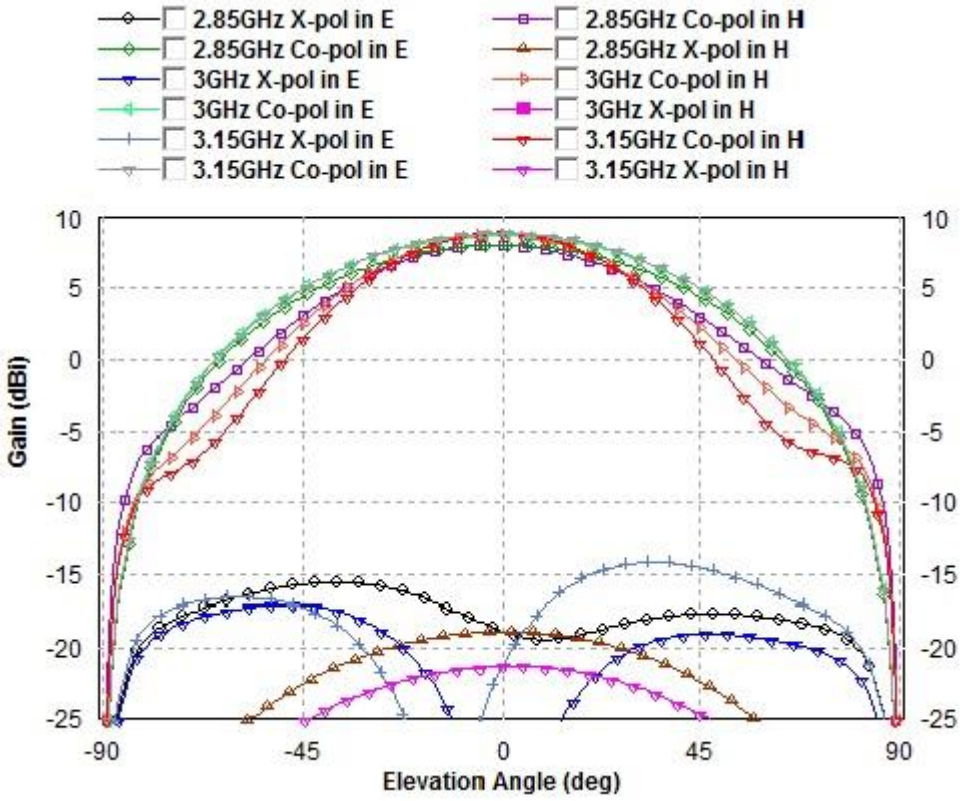

Fig. 19 Radiation Pattern of Patch Antenna with Four Transmission Lines

3.4 Single element patch antenna with the SP4T chips

3.4.1 Single Pole Four Throw RF Switch

The purpose of designing a circular patch antenna with four port is to excite a unique linear polarization. Herein, a single pole four throw RF switch is used in this design to active one of the four ports. The end of all the four transmission line are connected to driven patch, and the other ends are connected to a single pole four throw RF switch. We choose the SKY13322-375LF GaAs SP4T switch in this antenna design because of the low cost and great bandwidth. The Fig.20 is shown the switch layerout footprint. The size of this switch is 2mmX3mm. The width of each pin is 0.25mm [29].

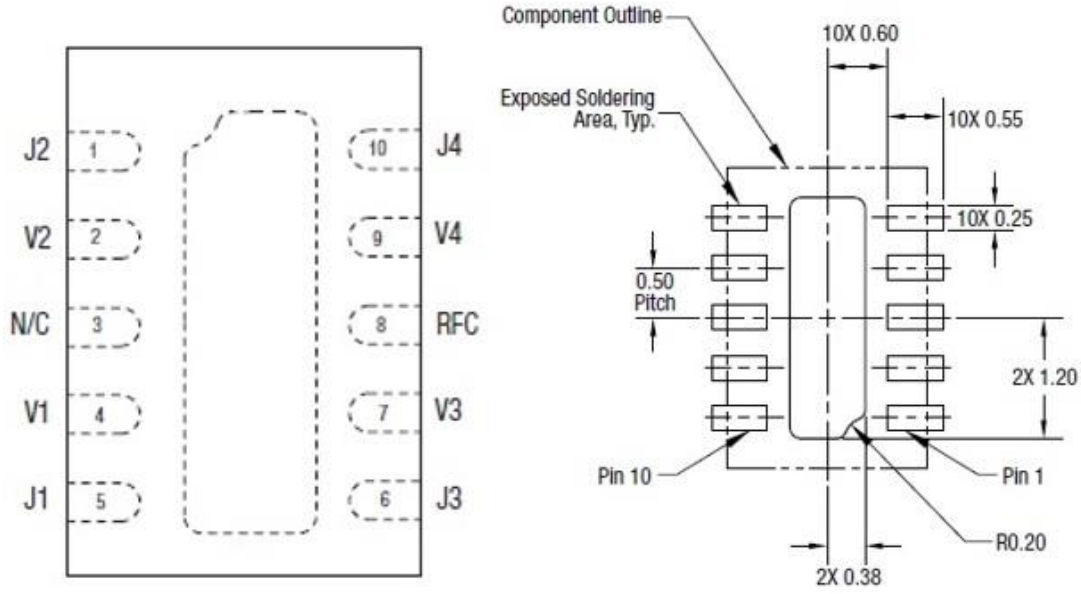

Fig. 20 Single Pole Four Throw RF Switch Layerout Footprint [29]

The four control pins as V1, V2, V3 and V4, determine only one of the four feeding lines is connected to the RF input. For example, if the control pin4 (V1) is connected to high voltage, the RF signal will go through pin5 (J1). The Table.2 is shown the SP4T switch truth table.

V1(Pin4)	V2(Pin2)	V3(Pin7)	V4(Pin9)	RFC to J1	RFC to J2	RFC to J3	RFC to J4
1	0	0	0	Insertion Loss	Isolation	Isolation	Isolation
0	1	0	0	Isolation	Insertion Loss	Isolation	Isolation
0	0	1	0	Isolation	Isolation	Insertion Loss	Isolation
0	0	0	1	Isolation	Isolation	Isolation	Insertion Loss

Table. 2 Single Pole Four Throw RF Switch Truth Table

3.4.2 Feeding Lines Design and Analysis

Considering the size of the switch, we need to design the feeding line instead of the straight transmission line to connect to the switch. The length of each feeding line is an integer times of half wavelength. Particularly, the feeding lines for Port 1 to Port 4 are one wavelength, one wavelength, 1.5 wavelengths and 3 wavelengths long, respectively. This guarantees that each inactive feeding line gives an open circuit at the edge of the driven patch, which produces minimum effects on both the return loss and the radiation characteristics for the excited port.

After optimizing the length of feeding line, the feeding line at port1 is designed at Fig.21 illustrated. The length of the feeding line at port1 is one wavelength as 54.557mm. The result of S11 is less than -28.8dB.

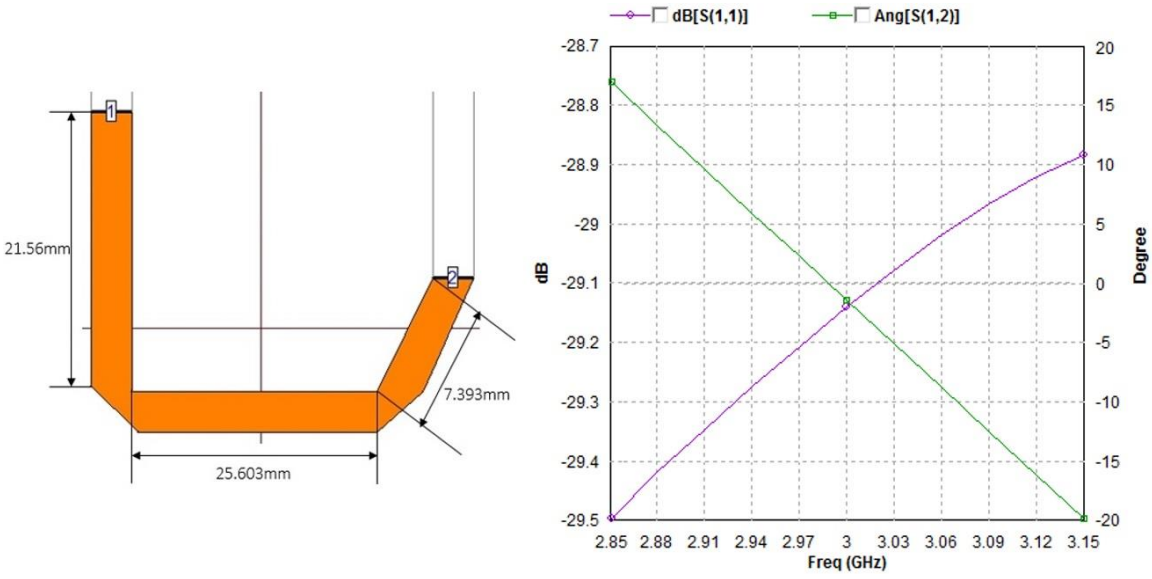

Fig. 21 Geometry and S11 Result of Feeding Line at Port1

The feeding line at port2 is designed at Fig.22 illustrated. The length of the feeding line at port2 is one wavelength as 51.9775mm. The result of S11 is less than -25.8dB.

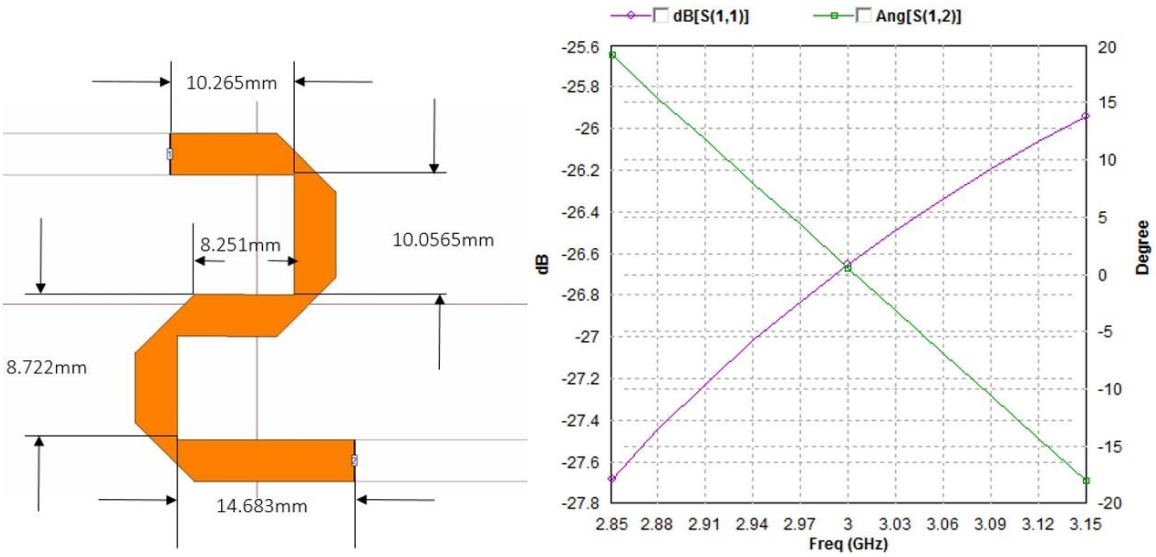

Fig. 22 Geometry and S11 Result of Feeding Line at Port 2

The feeding line at port3 is designed at Fig.23 illustrated. The length of the feeding line at port3 is one and half wavelengths as 89.97mm. The result of S11 is less than -27.5dB.

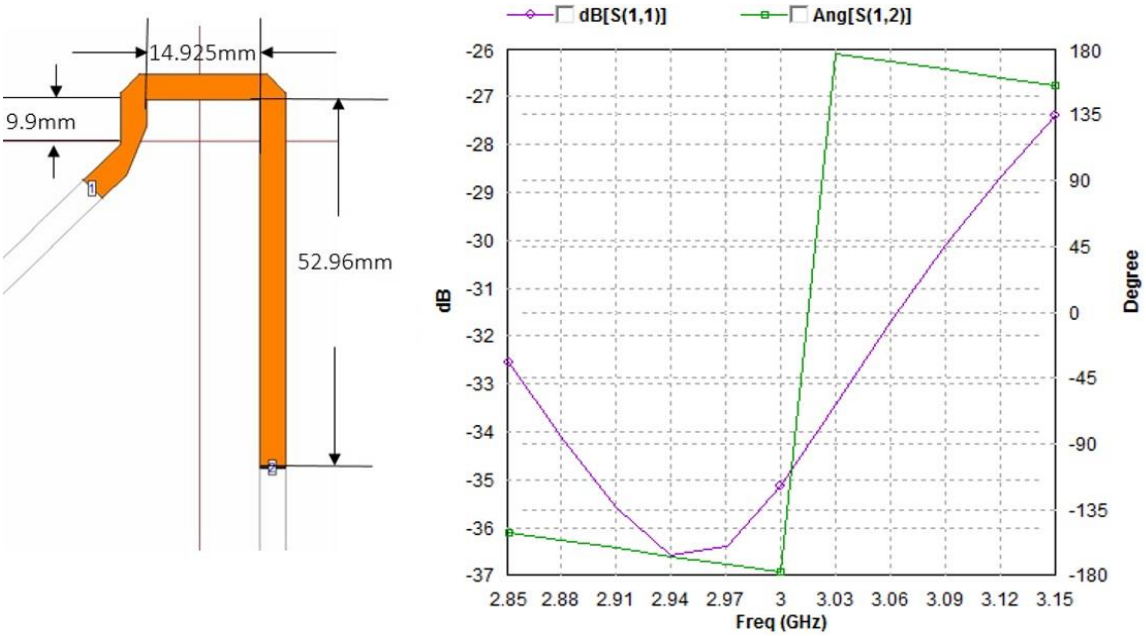

Fig. 23 Geometry and S11 Result of Feeding Line at Port 3

The feeding line at port4 is designed at Fig.24 illustrate. The length of the feeding line at port4 is three wavelengths as 176.98mm. The result of S11 is less than -18dB.

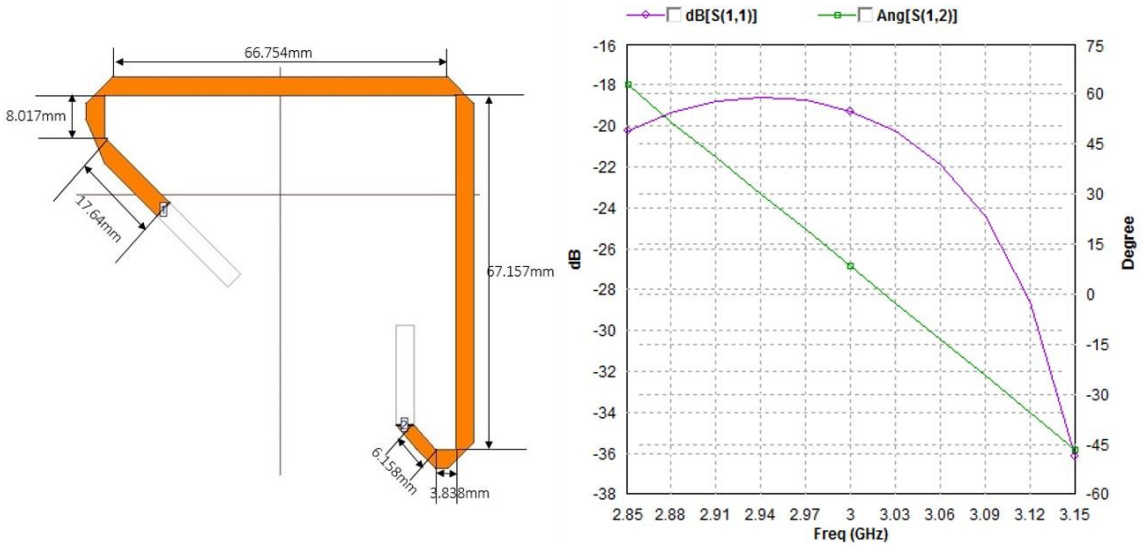

Fig. 24 Geometry and S11 Result of Feeding Line at Port 4

3.4.3 RF Feeding Line Design and Analysis

From the Fig.20, we can see the pin8 is the RF feeding port. The RF signal is fed to single pole four throw RF switch at pin8, then the four control pins will determine which port is excited to implement the linear polarization. The size of the pin8 is very tiny as 0.55mmX0.25mm. We design the RF feeding line as one end width of 0.5mm and the other width of 1mm. The end of 0.5mm width is connected to RF switch, and the end of 1mm width is connected to the power divider.

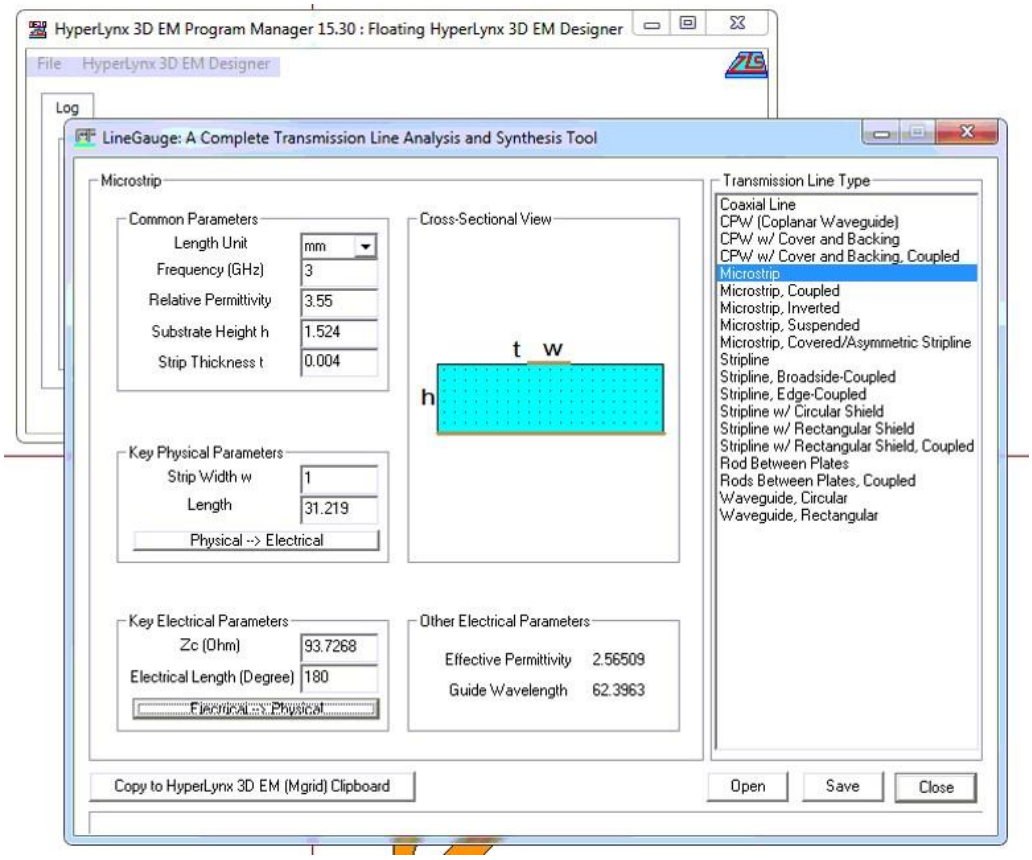

Fig. 25 RF Feeding Line Calculation in IE3D

The Fig.25 is illustrated the RF feeding line size calculation by using LineGauge in IE3D. The length of RF feeding line should be half wavelength as 31.219mm. The impedance of RF feeding line is around 100Ω. Then, we construct the RF feeding line as Fig.26 illustrated.

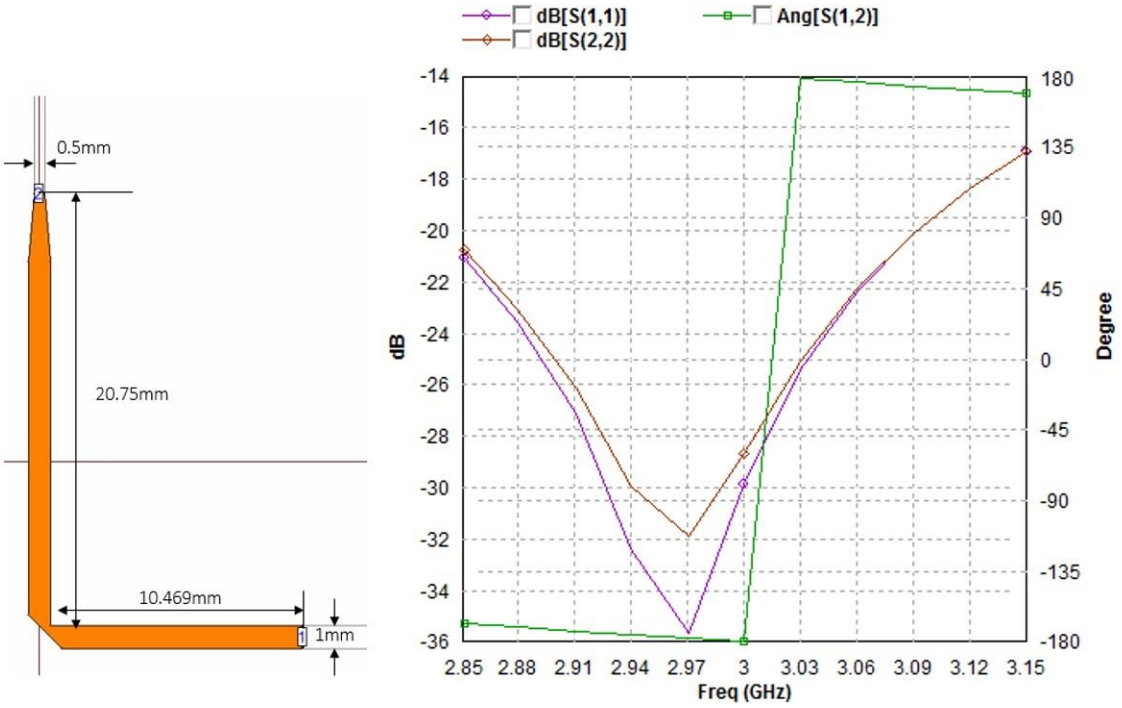

Fig. 26 Geometry and S11 of RF Feeding Line

During the simulation process, we need to setup the load impedance as 100Ω, to guarantee the impedance matching. As the Fig.26 shown, the results of reflection coefficient S11 and S22 are both less than -17dB in RF feeding line. The reflection coefficient at port1 is defined S11, and the reflection coefficient at port 2 is defined S22.

3.4.4 Reconstruct the Patch Antenna with the Four Feeding Lines

The reflection coefficient results of the four port feeding illustrated in Fig.21 to Fig 24 are satisfy to the goal. The return loss of better than 14dB can be observed from 2.85GHz to 3.75GHz for the four port feeding lines. Then, the single element patch antenna could be reconstructed with those four feeding lines as illustrated in Fig.27.

The port1 feeding line is connected to driven patch in vertical direction. The port2 feeding line is in horizontal direction. The port3 and port4 feeding lines are located at ±45˚ with the y axis, respectively. The other ends of feeding lines is connected with single pole four throw RF switch. The switch location is illustrated in Fig.27 with the size of 2.2533mmX2.293862mm.

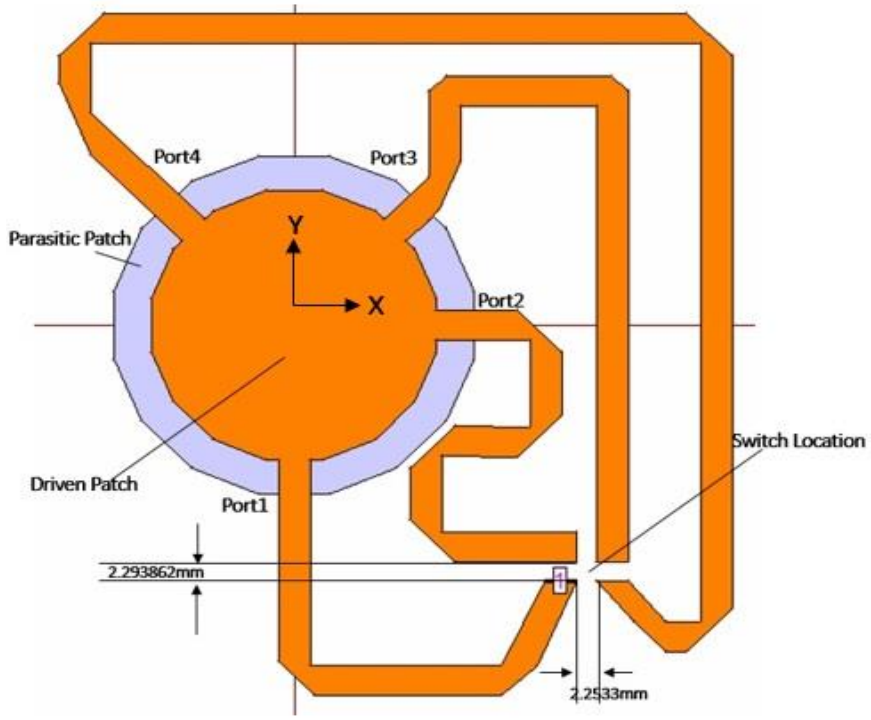

Fig. 27 Geometry of Patch Antenna with Four Feeding Lines

Then, we excite one port, and make the other three ports as open circuit to simulate this single element patch antenna. The reflection coefficient is illustrated in Fig.28 to Fig.31.

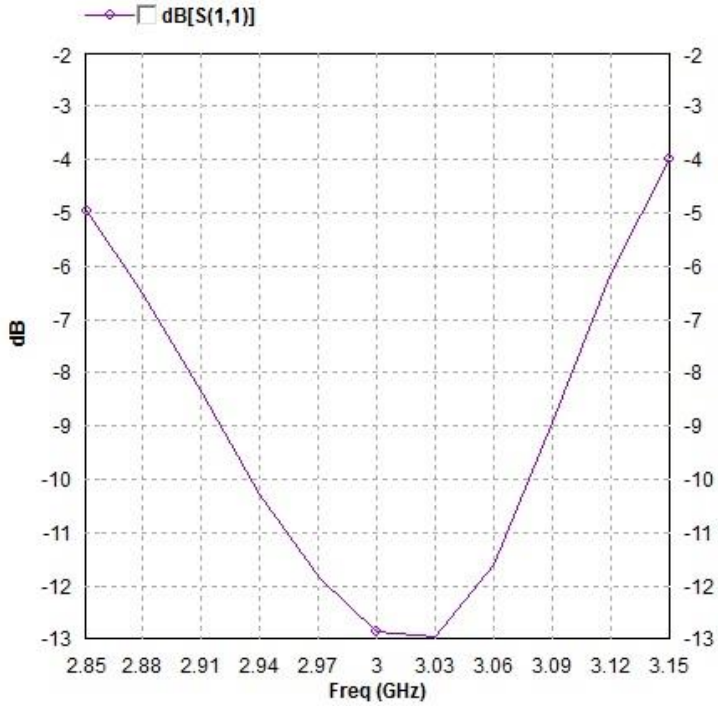

Fig. 28 S11 Result of Patch Antenna at Port 1

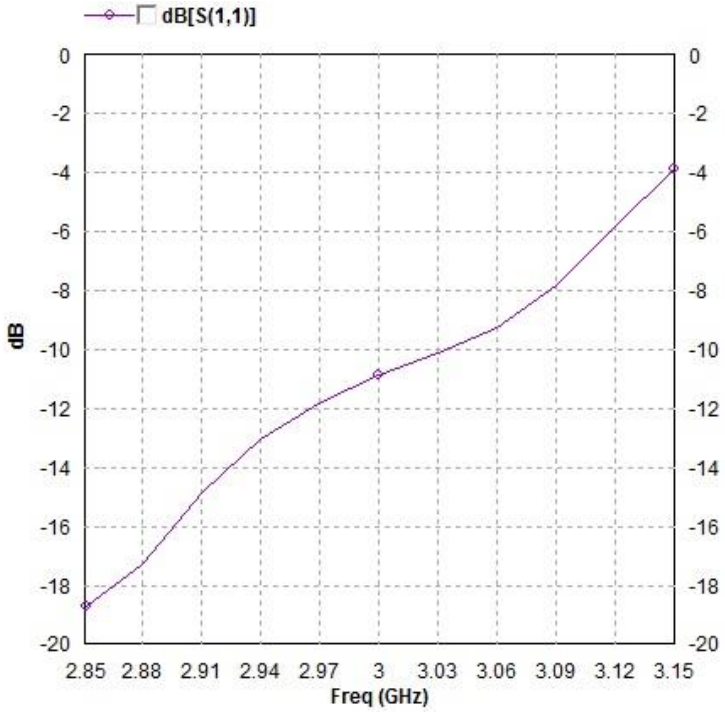

Fig. 29 S11 Result of Patch Antenna at Port 2

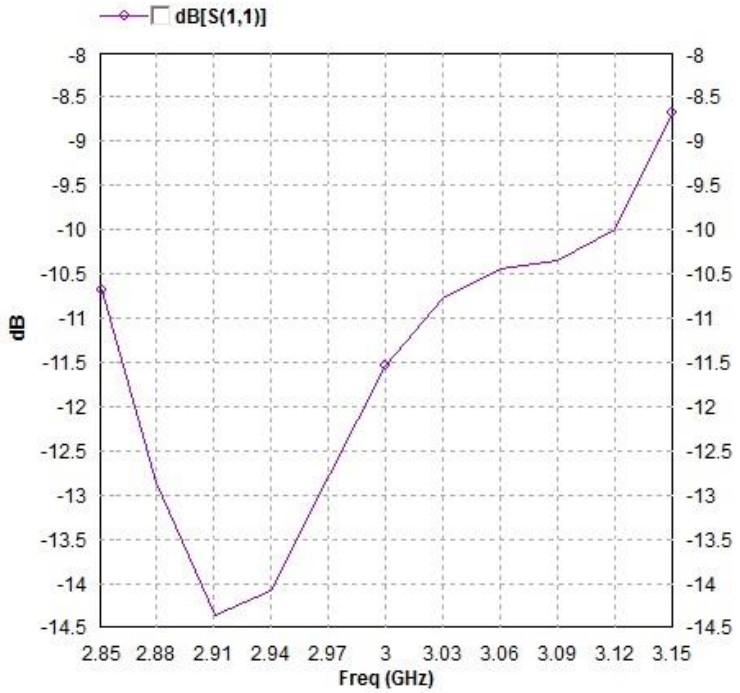

Fig. 30 S11 Result of Patch Antenna at Port 3

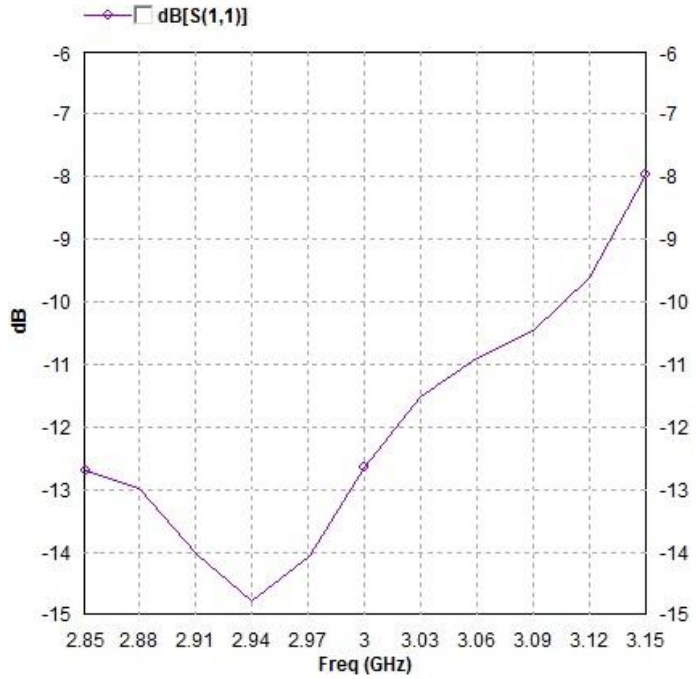

Fig. 31 S11 Result of Patch Antenna at Port 4

The results of reflection coefficient illustrated in Fig.28 and Fig29 are not good performance. The reflection coefficient results of port1 observed from 2.938GHz to 3.085GHz is less than -10dB. The reflection coefficient of port2 is so bad at high frequency region. As the Fig.30 and Fig.31 shown, the reflection coefficient results of port3 and port4 are satisfy to -10dB between the frequency of 2.85GHz to 3.12GHz. Herein, we need redesign the feeding line of each ports.

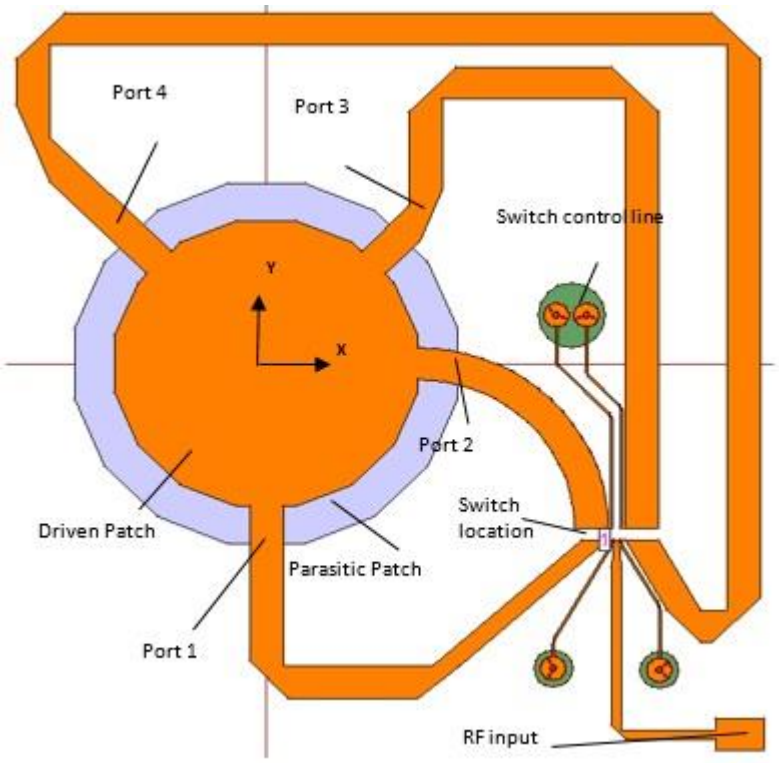

Fig. 32 Geometry of Patch Antenna with Four Ports and RF Feeding Line

As Fig.32 shown, the feeding lines for Port 1 to Port 4 are one wavelength, half wavelength, 1.5 wavelengths and 3.5 wavelengths long, respectively. Also the RF feeding lines and switch control lines are added to the driven patch. Then, we excite

one port only and the rest ports are open circuits at the ends that connect to the RF switch. The simulated reflection coefficient results is illustrated in Fig.33 to Fig.36, and the simulated radiation pattern results is shown in Fig.37 to Fig.40.

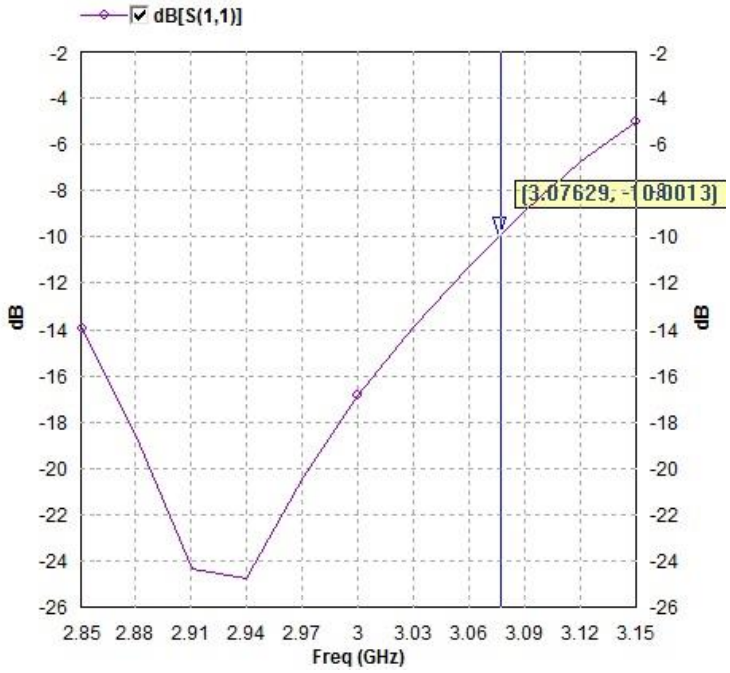

Fig. 33 S11 Result of Patch Antenna with Four Ports and RF Feeding Line at Port1

The simulated resluts of reflection coefficient at port 3 and port 4 are less than -10dB at the frequency between 2.85GHz to 3.12GHz. But the results at port1 and port2 are still not good enough. For S11 lower than -10dB, the frequency band at port 1 is between 2.91GHz to 3.1GHz, and the frequency band at port 2 is between 2.85GHz to 3.075GHz. So we change the observation region from 2.91GHz to 3.075GHz.

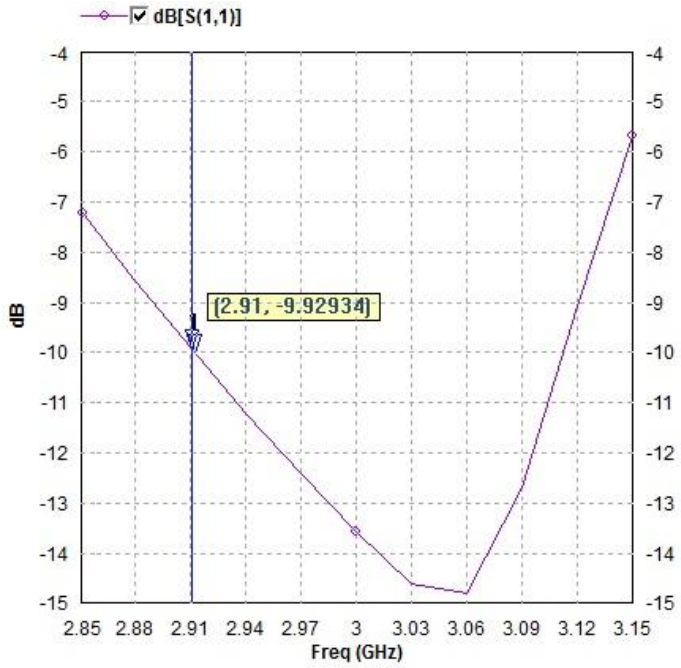

Fig. 34 S11 Result of Patch Antenna with Four Ports and RF Feeding Line at Port2

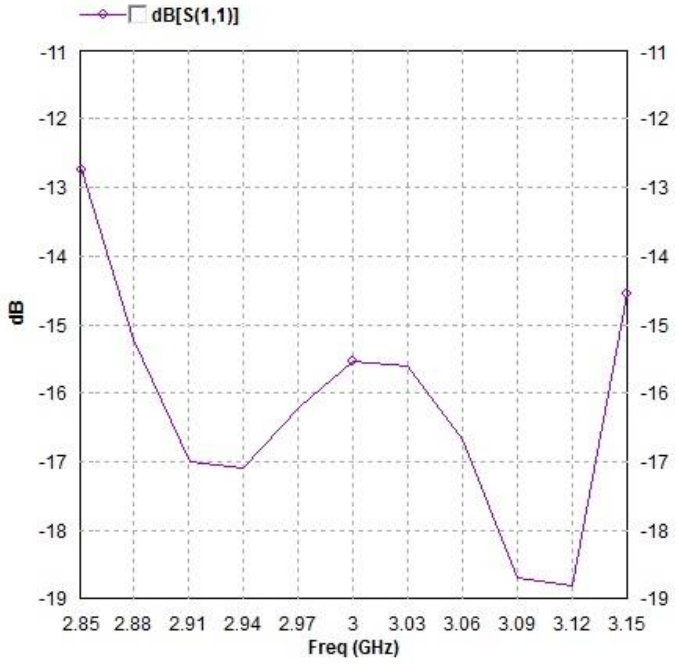

Fig. 35 S11 Result of Patch Antenna with Four Ports and RF Feeding Line at Port3

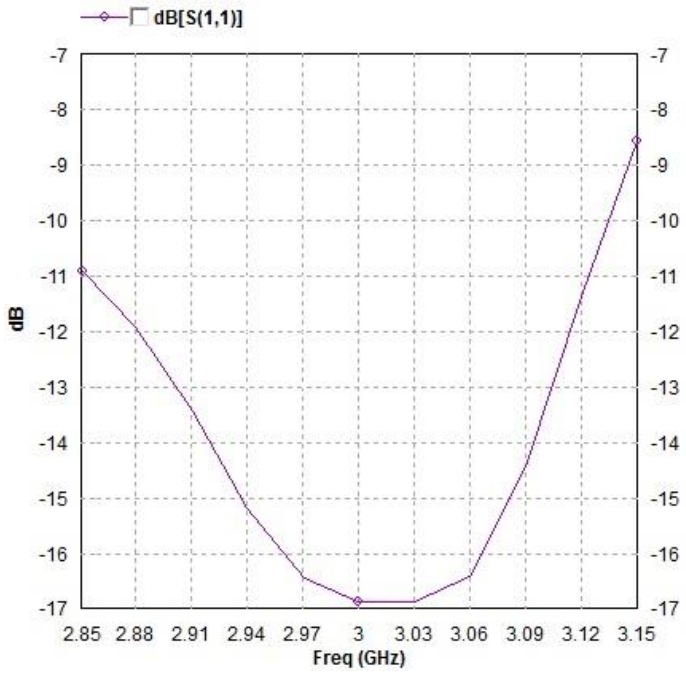

Fig. 36 S11 Result of Patch Antenna with Four Ports and RF Feeding Line at Port4

Radiation patterns in the two principle planes are plotted in Fig. 37 to Fig. 40, for Port 1 to Port 4, respectively. It can be seen that all the four polarizations has a gain value of around 8dB. The cross-pol discrimination in the broadside direction is around 15dB for Port 1 to Port 4. Clearly, the inactive feeding lines does not significantly affect the polarization purity of the active feeding port.

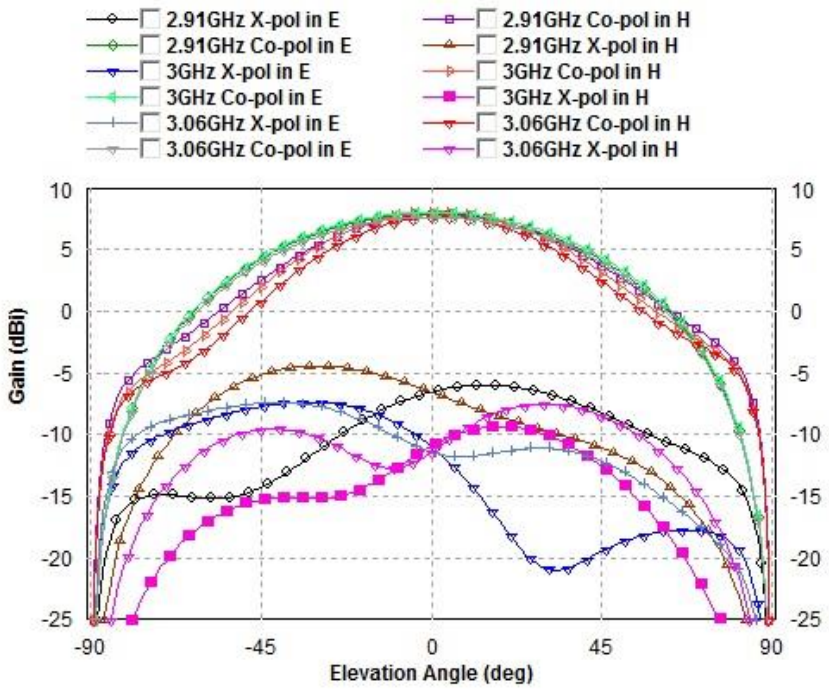

Fig. 37 Radiation Pattern of Patch Antenna with Four Ports and RF Feeding Line at Port1

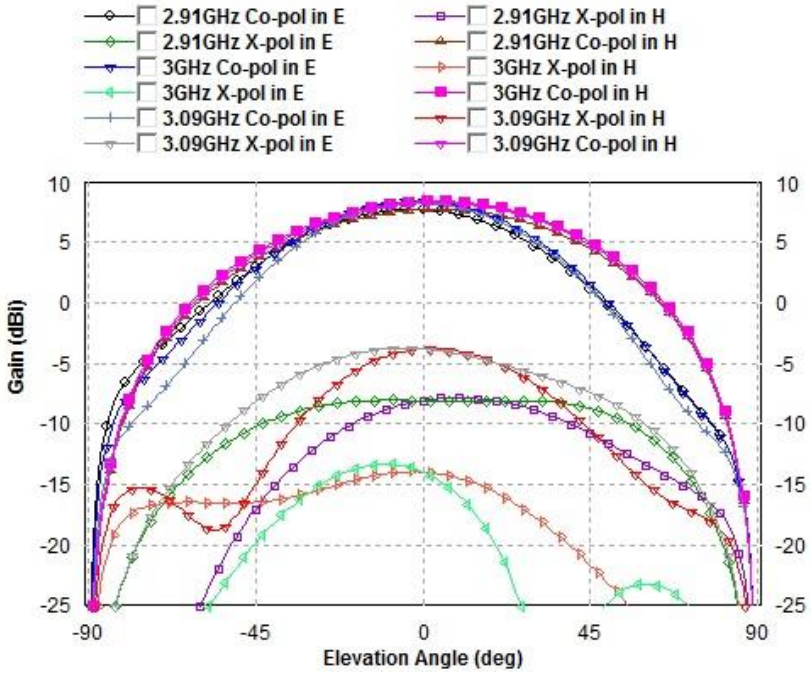

Fig. 38 Radiation Pattern of Patch Antenna with Four Ports and RF Feeding Line at Port2

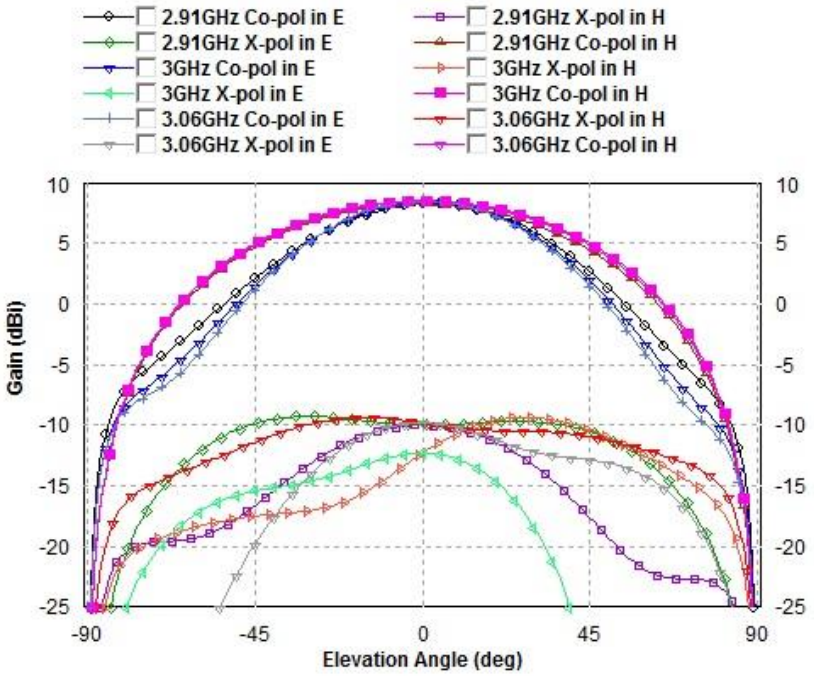

Fig. 39 Radiation Pattern of Patch Antenna with Four Ports and RF Feeding Line at Port3

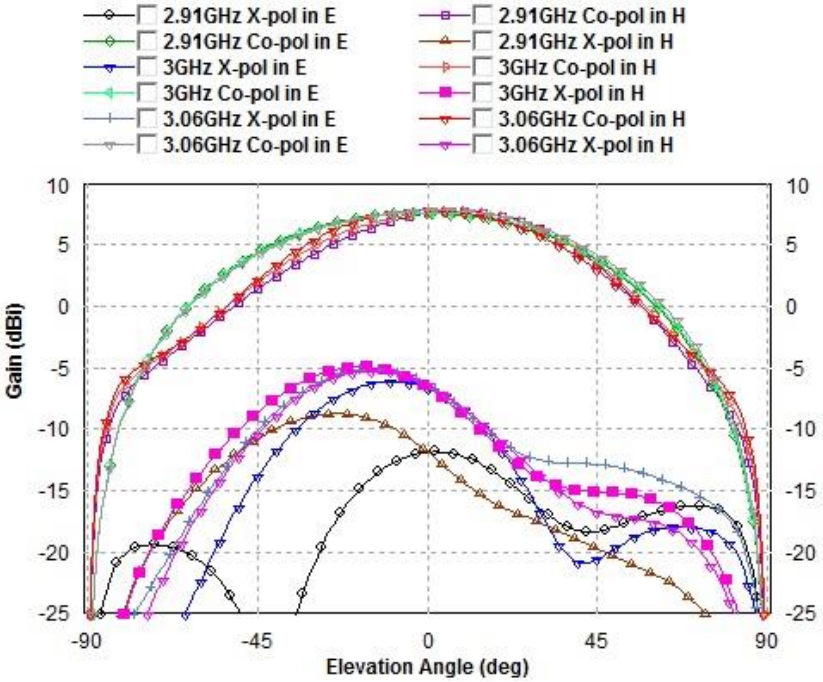

Fig. 40 Radiation Pattern of Patch Antenna with Four Ports and RF Feeding Line at Port4

3.5 Power Divider Design

For this research, we need to design a 2X2 antenna array to improve the gain performance. The power divider should be designed to divide the RF signal to transmit to each antenna element [30]. First of all, we need to determine the distance between the two antenna elements. The distance should be less than one wavelength, so we choose 90mm between the two antenna elements.

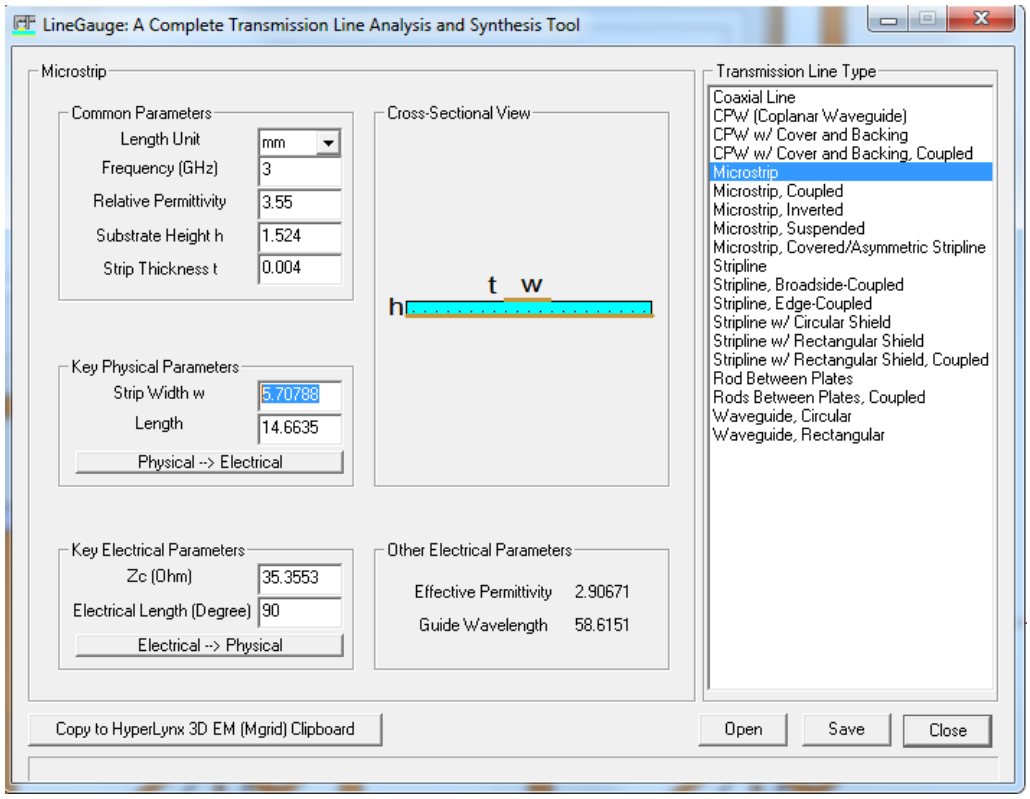

Fig. 41 1X2 Antenna Arrays Power Divider Calculation in IE3D

The end of power divider should be connected to the RF feeding line and a 50Ω impedance transmission line. Basic on the transmission line theory [31], we can calculate the impedance of the divider $Z_M = \sqrt{50 \cdot 25} = 35.355\Omega$. LineGauge in IE3D

can calculate the size of the divider as shown in Fig.41. The geometry of power divider with 1X2 Antenna Arrays is illustrated in Fig.42. The size of the divider is 14.6mmX5.7mm.

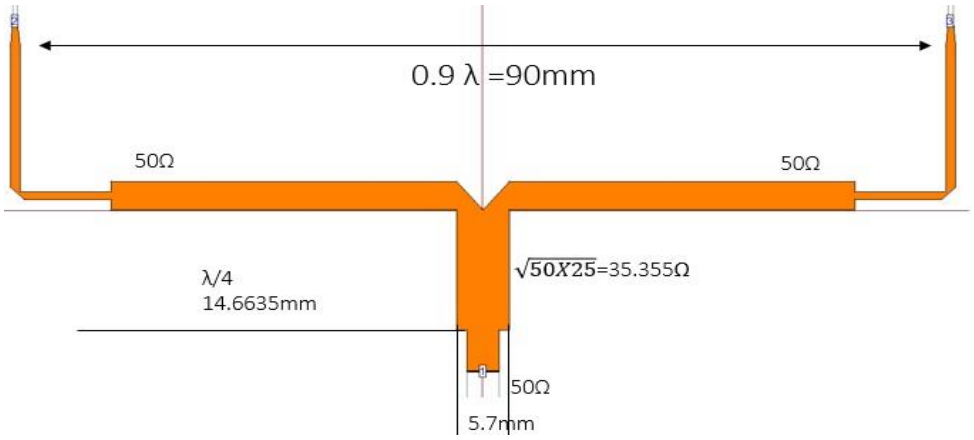

Fig. 42 Geometry of 1X2 Antenna Arrays Power Divider

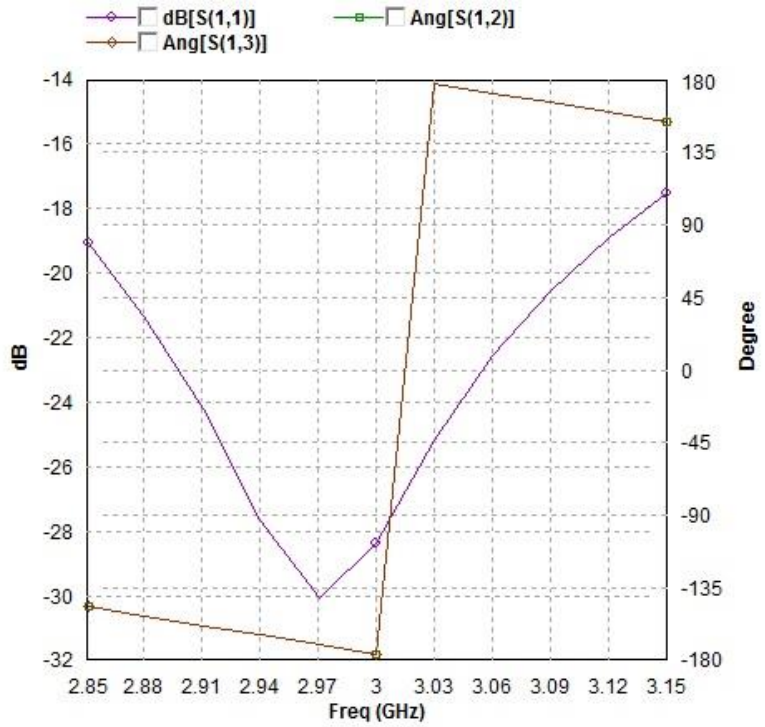

Fig. 43 S11 Result of 1X2 Antenna Arrays Power Divider

The simulated result of reflection coefficient at port1 is shown in Fig.43. The S11 value is less than -17dB in the frequency region between 2.85GHz and 3.15GHz.

For this 2X2 antenna array, we choose to use SAM adapter to feed RF signal to this antenna array [32]. As we known, the SAM adapter impedance is 50Ω. The RF signal is divided to the two transmission lines with 50Ω impedance. So the center transmission line impedance of 2X2 antenna array power divider should be calculated as $Z_M = \sqrt{50 \cdot 100} = 70.71\Omega$. The center transmission line size of 2X2 antenna array power divider can be calculated by using LineGauge in IE3D as Fig.44 illustrated.

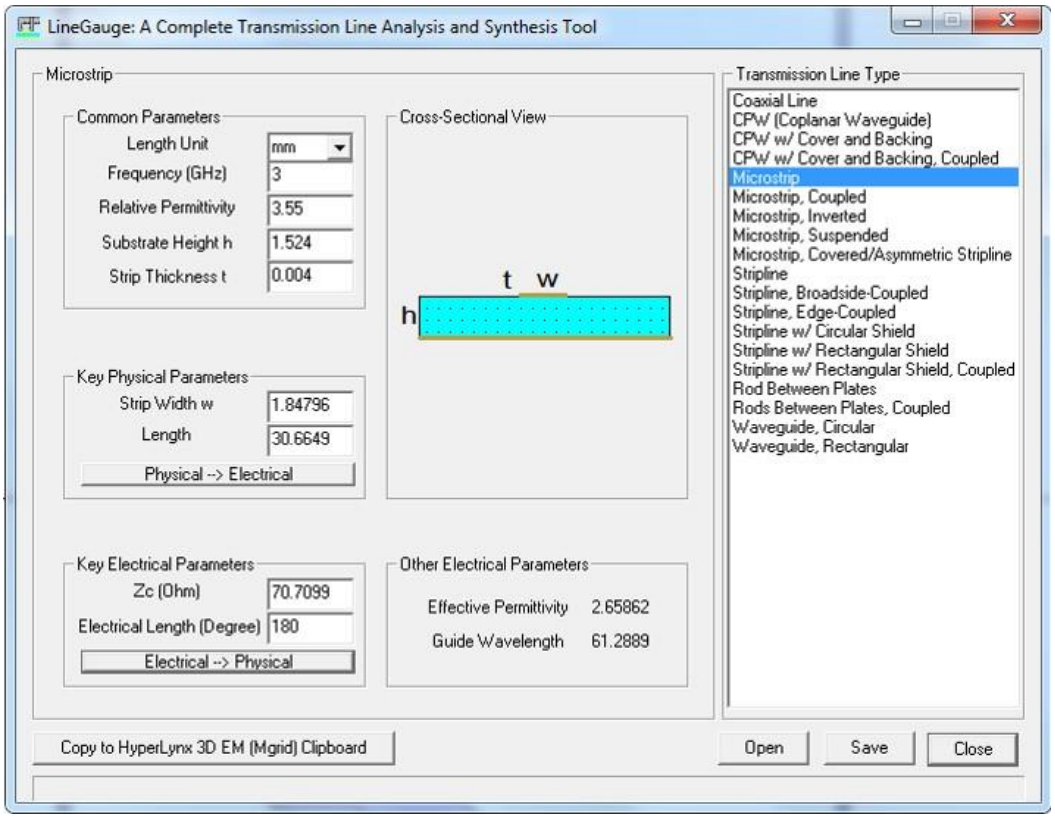

Fig. 44 2X2 Antenna Array Power Divider Calculation in IE3D

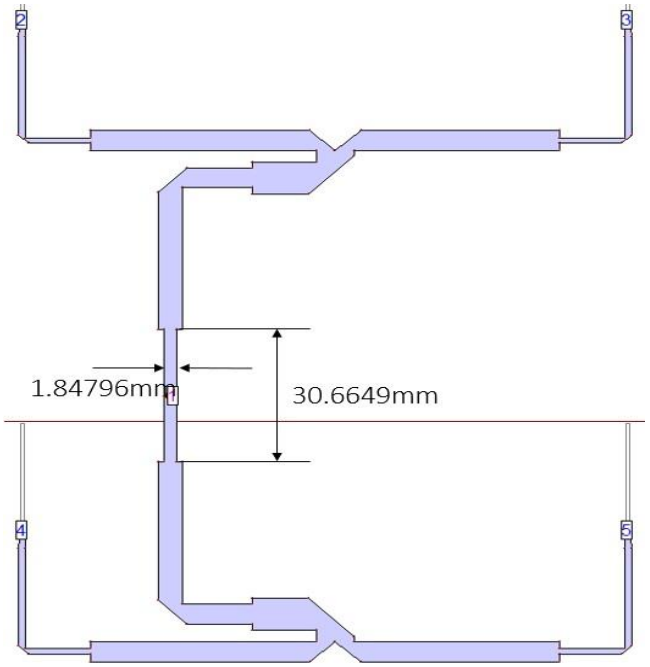

Fig. 45 Geometry of 2X2 Antenna Array Power Divider

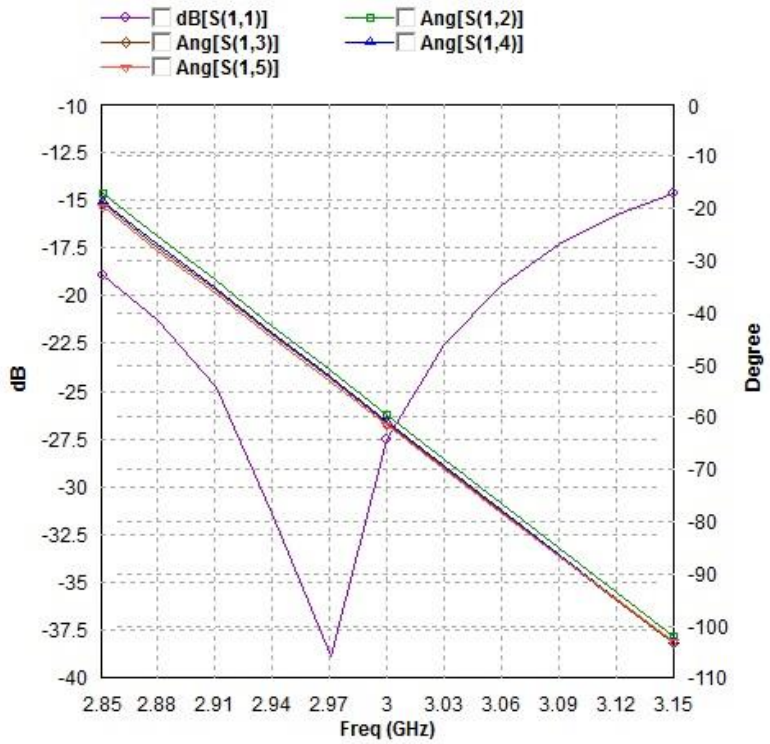

Fig. 46 S11 Result of 2X2 Antenna Array Power Divider

The 2X2 antenna array power divider geometry is constructed in IE3D as the Fig.45 shown. The size of center transmission line is 30.6649mmX1.84796mm. This power divider can divide the RF signal to the four antenna elements. Then, we add a port at the center transmission line to simulate this power divider. The simulated resluts S11 of the power divider is less than -17dB at the frequency region between 2.85GHz to 3.12GHz. This S11 result is good enough for this desgin, but we should know we cannot add a SAM port in IE3D. The result S11 shown in Fig.46 is a simulation without a SAM adapter. So we try to use HFSS to simulate this power divider with a SAM adapter. The Fig.47 is illustrated the geometry of 2X2 antenna array power divider with SAM adapter in HFSS. After optimation and simulation, the size of center transmission line is changed to 33.744mmX1.779mm. The simulated reflection coefficient is also satisfy to the goal as Fig.48 shown, and the whole 2X2 polarization switchable patch antenna array is shown as Fig.49 with size of 166.73mmX107.46mm.

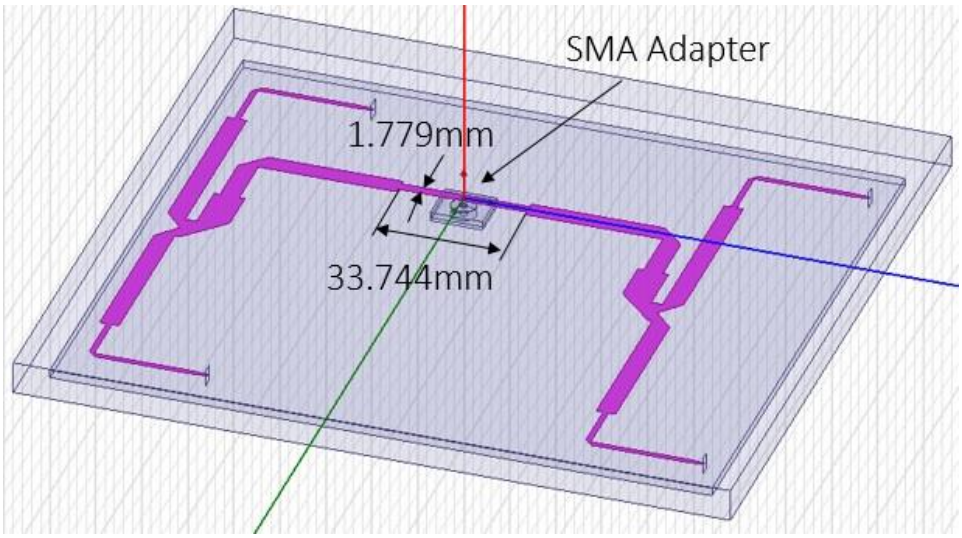

Fig. 47 Geometry of 2X2 Antenna Array Power Divider in HFSS

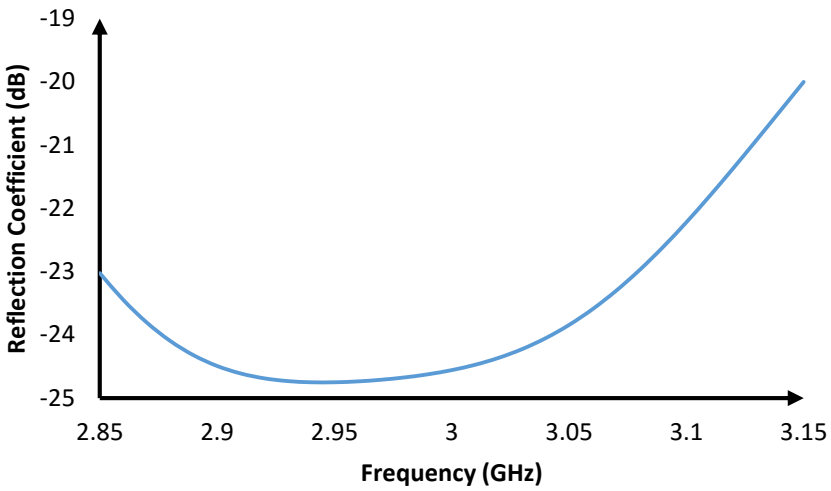

Fig. 48 S11 Result of 2X2 Antenna Array Power Divider in HFSS

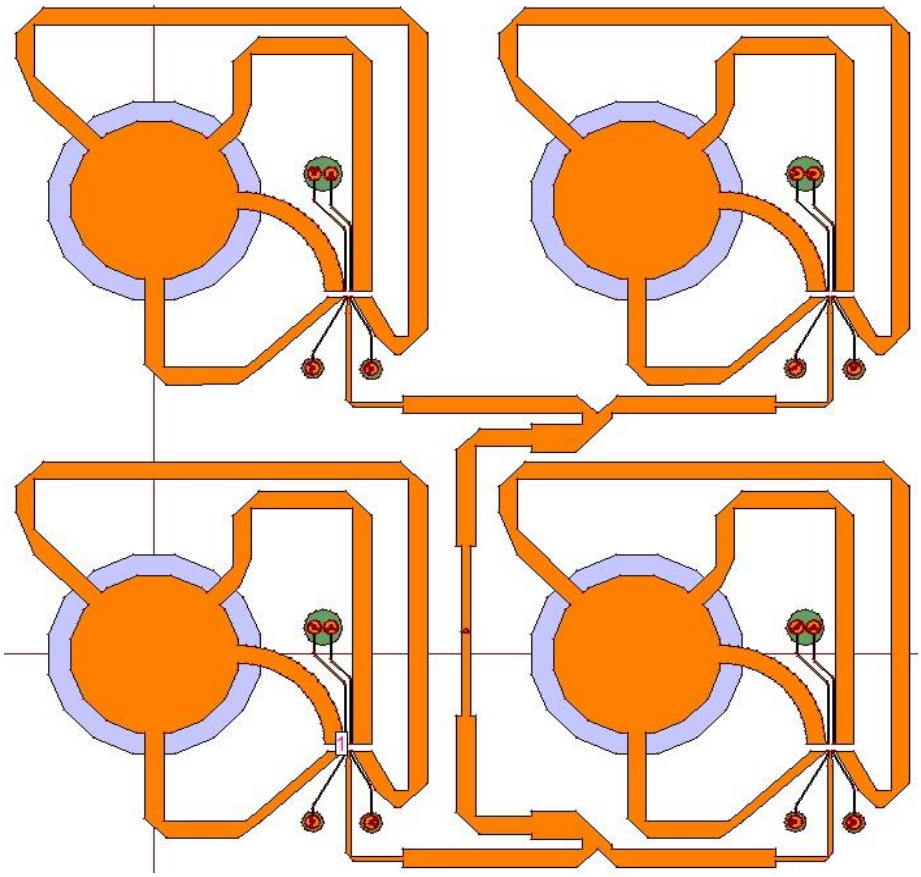

Fig. 49 Geometry of 2X2 Patch Antenna Array

Chapter 4 Antenna Measurement

Considering the time shortage, I only fabricate the single element patch antenna with four straight transmission lines. The Fig.50 is shown the fabrication prototype of the driven patch and parasitic patch. The four ports are printed on the driven patch as microstrip transmission lines. Each port is connected with SMA adapter.

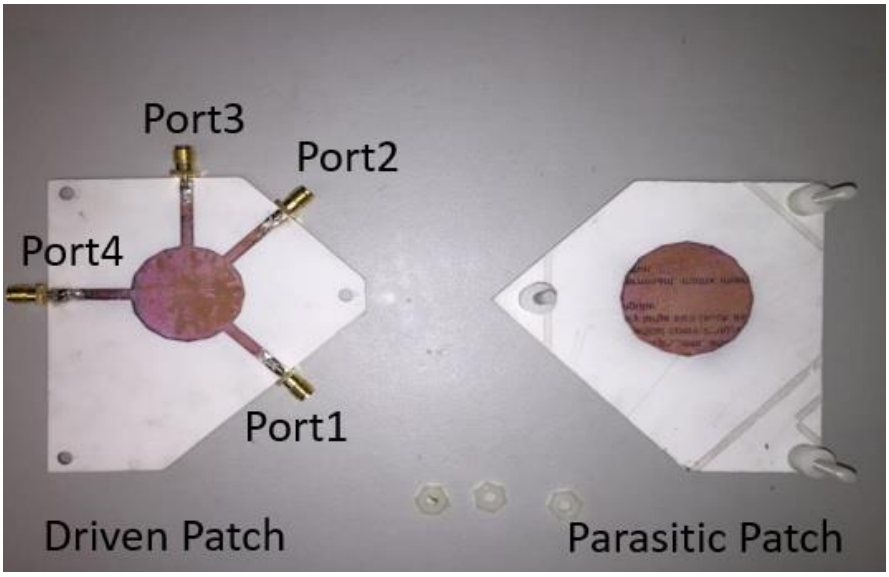

Fig. 50 The Fabrication Prototype of Single Element Patch Antenna

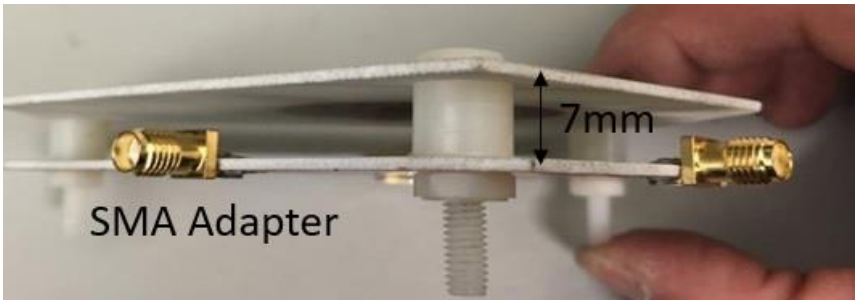

Fig. 51 The Fabrication Prototype of Single Element Patch Antenna

The Fig.51 is illustrated the construction of the single element patch antenna. The distance between the driven patch and parasitic patch is 7mm.

4.1 Return Loss Measurement

In our Antenna Lab, we use the Wiltron 360B Vector Network Analyzer to measure the return loss and gain of the single element patch antenna. As Fig.52 shown, one port is connected with vector network analyzer, and RF signal excites this port. Then we can read the result of return loss from the screen as -10dB at the frequency bandwidth from 2.9GHz to 3.1GHz.

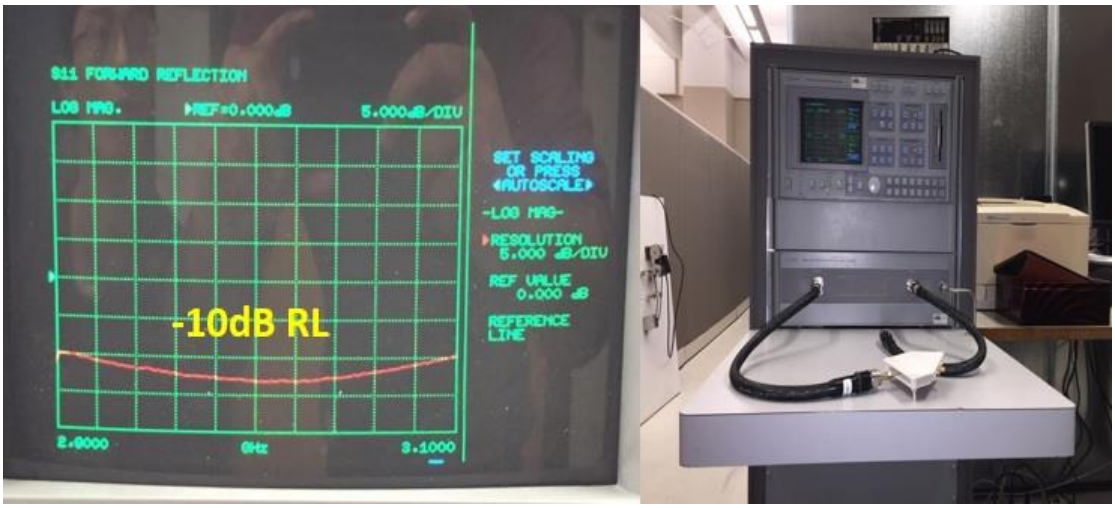

Fig. 52 Return Loss Measurement in Wiltron 360B Vector Network Analyzer

4.2 Gain Measurement

The Gain is usually measured by using gain comparison method. An antenna of known gain, called a standard gain antenna, is used to refer to the test antenna gain [33]. Initially, the 10dB standard gain horn antenna should be placed in anechoic chamber. The transmitter of fixed input power P_t is connected to a suitable source antenna. The received power in standard gain horn antenna can be measure as P_S. Next, we replace the test antenna at receiving side as Fig.53 shown. Then, the test antenna received

power can be measured at P_T. The gain of the test antenna can be calculated from the gain of the standard gain horn antenna [34] by

$$G_T = \frac{P_T}{P_S} G_s$$

This equation can be compressed in decibels:

$$G_T(dB) = P_T(dBm) - P_S(dBm) + G_s(dB)$$

Where G_T is the test antenna gain, P_T is measured RF signal power of test antenna, P_S is the measured RF signal power of standard gain horn antenna, and G_s is the gain of standard gain horn antenna as 10dB.

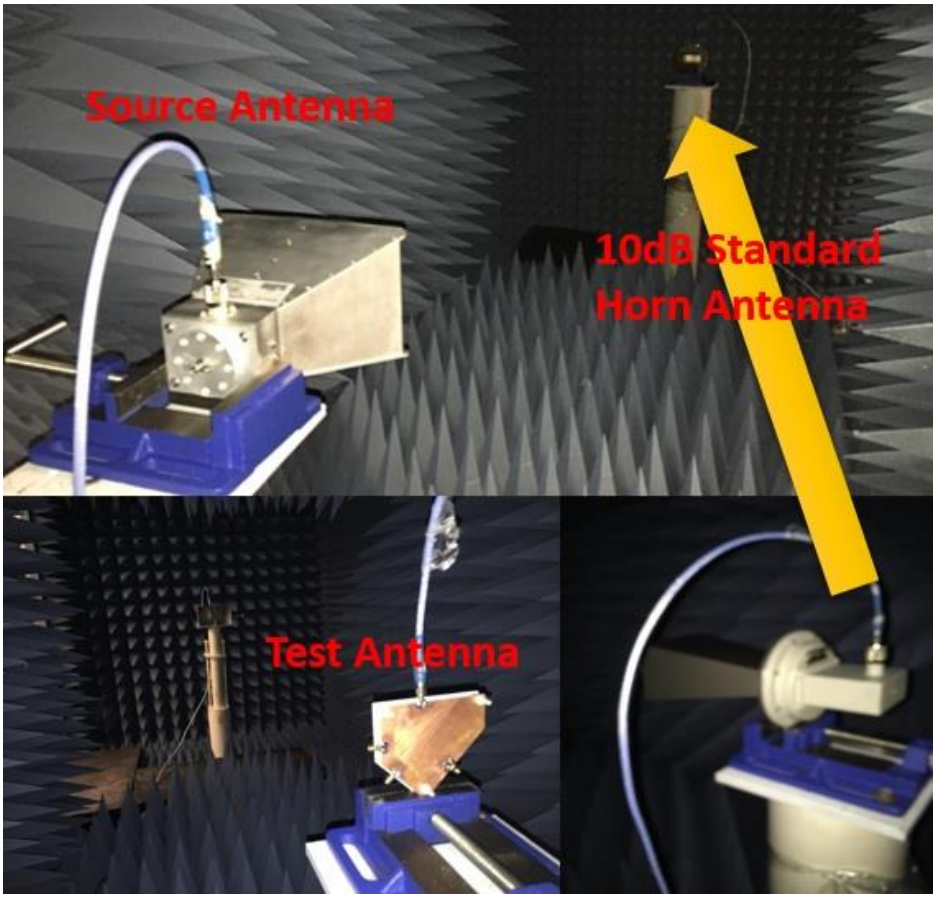

Fig. 53 Gain Measurement in Anechoic Chamber

The gain result of the single element patch antenna is shown in Fig.54 as 7dB at the frequency bandwidth from 2.9GHz to 3.1GHz. Then, we use the same method to measure each port, and the result is also around 7dB at the frequency bandwidth from 2.9GHz to 3.1GHz. Comparing to the simulated result, this single element patch antenna is good performed in this frequency bandwidth.

Fig. 54 Gain Measurement Result

Chapter 5 Conclusion

The properties and development of a four-port circular patch antenna array for polarization modulation have been studied in this work. Initially the theory of patch antenna and polarization modulation related to this work is introduced. According to this concept, a four-port circular patch antenna array was designed for point to-point wireless communications using polarization modulation scheme. The feeding lines for all the four ports are connected to an RF switch for the operation of polarization modulation. In order to minimize the effects of inactive feeding lines on the return loss and radiation characteristics for the active polarization, all the feed lines have a length that equals to an integer times of half wavelength. Finally, simulation is carried out and shows good return loss and polarization purity for all the four ports. The advantage for this antenna are low cost and easily fabrication. Also, bit rate can be increased without additional bandwidth or transmission power. But, the low gain and low impedance bandwidth are the disadvantage for this patch antenna array.

Considering the time shortage, we only finish the measurement of the reflection coefficient and gain for single element patch antenna. And also, we have already send the four-port circular patch antenna array to the company to fabricate. Later on, we will continue to measure and develop this antenna to improve the implementation.

Reference

[1] Sergio Benedetto and Pierluigi Poggiolini, “Theory of polarization shift keying modulation”, IEEE Transactions on communications, Vol.40, No.4, April 1992.

[2] Foschini,Gerard J, “Layered space-time architecture for wireless communication in a fading environment when using multi-element antennas”, Bell Labs Technical Journal, Vol 1, Issue 2, pp. 41-59, Autumn, 1996.

[3] Parihar M.S, Basu A, Koul S.K, “Polarization reconfigurable microstrip antenna”, Microwave Conference, IEEE, pp.1918-1921, Dec. 2009

[4] B.J. Kwaha, O.N Inyang and P. Amalu. “The circular microstrip patch antenna design and implementation”, IJRRAS,Vol8, pp.1-2, July 2011.

[5] Warren L. Stutzman and Gary A. Thiele. “Antenna theory and design third edition”, John Wiley & Sons, Inc. 2013.

[6] K.V Rop and D.B.O. Konditi. “Performance analysis of a rectangular microstrip ptach antenna on different dieletric substrats” Innovative Systems Design and Engineering, Vol.3, No.8, pp.1727-1729, 2012.

[7] Patch Antennas, Microstrip Antennas, [online] http://www.antenna-theory.com.

[8] Jeffrey Frank Jones, “Electronic warfare and radar systems engineering handbook”, Naval Air warfare center weapons division point MUGU, California, pp.3-3.1, 2012.

[9] Kirk T. McDonald, “Electrodynamics Problem Set 4”, Princeton University, 1999.

[10] G.H. Huff and J.T. Bernhard,"Integration of packaged RF MEMS switches with radiation pattern reconfigurable square spiral microstrip antennas", IEEE Transaction on antennas and propagation, Vol 54, Issue 2, pp.464-469, 2006.

[11] C.A. Balanis, "Antenna theory: a review", Proceedings of the IEEE, Vol 80, Issue 1, pp.7-23, 1992.

[12] Bhalla R and Shafai, "Broadband patch antenna with a circular arc shaped slot", IEEE antenas and propagation society international symposium, pp.394-397, 2002.

[13] E.R. Brown and C.D. Parker, "Radiation properties of planar antenna on a photonic-crystal substrate", J Opt Soc Am B, Vol 10, No.2, 1993.

[14] Rod Waterhouse, "Printed antennas for wireless communications" John Wiley & Sons Ltd, West Sussex, England, 2007.

[15] R. Gonzalo and B. Martinez, "The Effect of Dielectric Permittivity on the Properties of Photonic Band Gap Devices," Microwave and Optical Technology Letters, vol. 23, 1999.

[16] M. Tanaka and J.-H. Jang, "Wearable mircostrip antenna," IEEE Antennas and Propagation Society International Symposium, pp. 704-707, vol. 2, Jun. 22-27, 2003.

[17] David M. Pozar, "Microwave engineering fourth edition", John Wiley & Sons Inc, pp. 56-60, 2012.

[18] B.P. Lathi, "Modern digital and analog communication systems fourth edition", Oxford University press, pp.178-230, 2009.

[19] Gardner F.M., “A BPSK/QPSK timing-error detector for sampled receivers”, IEEE Transactions on Communications, Vol 34, pp. 423-429, 1986.

[20] BPSK, [online] www.kprblog.in.

[21] N.S. Alagha, “Cramer-Rao bounds of SNR estimates for BPSK and QPSK modulation signals”, IEEE Communications Letters, 2001.

[22] Marco Romagnoli, M.D. Levenson, and G.C. Bjorklund, “Frequency-modulation-polarization spectroscopy”, Opt. Lett, Vol 8, Issue 12, pp. 635-637, 1983.

[23] A. Carena, V. Curri, R. Gaudino, N. Greco, P. Poggiolini and S. Benedetto, “Polarization modulation in ultra-long haul transmission systems: a promising alternative to intensity modulation”, Optical Communication European Conference, Vol. 1, pp. 429-430, 1998.

[24] E. Lier, D. Purdy, J. Ashe and G. Kautz, “An On-Board Integrated Beam Conditioning System for Active Phased Array Satellite Antennas," 2000 IEEE Intern. Conf. on Phased Array Systems and Technol, pp. 509 - 512, 2000.

[25] D. Purdy, J. Ashe, E. Lier, US Patent: 2002/0171583 A1, “System and Method for Effciently Characterizing the Elements in an Array Antenna," Nov. 21, 2002.

[26] Rogers Corporation, [online] www.rogerscorp.com.

[27] Mentor Graphics Inc. HyperLynx 3D EM, [online] www.mentor.com

[28] Christophe Caloz and Tatsuo Itoh, “Electromagnetic Metamaterials Transmission Line Theory and Microwave Application”, John Wiley & Sons, Inc. 2006.

[29] Skyworks Solution, Inc. SKY13322-375LF, [online] www.skyworksinc.com

[30] Lars Josefsson and Patrik Persson, “Conformal Array Antenna Theory and Design”, IEEE Antennas and Propagation Society, Sponsor, John Wiley and Sons, Ltd., Hoboken, New Jersey, 2006.

[31] Mongja Rajesh, Bahl Inder J and Bhartia Prakash, “RF and Microwave coupled-line circuits”, Artech House microwave library, 1999.

[32] D. J. Chung, S. K. Bhattacharya, G. E. Ponchak and J. Papapolymerou, “An 8x8 lightweight exible multilayer antenna array," Proc. IEEE Antennas Propag. Soc. Int. Symp. Dig., June 1-5, 2009.

[33] Hsin Chia Lu and Tah Hsiung Chu, “Antenna gain and scattering measurement using reflective three antenna method”, IEEE Antennas and Propagation Society International Symposium, Vol 1, pp. 374-377, 1999.

[34] R. Przesmycki, M. Wnuk, L. Nowosielski, K. Piwowarczyk and M. Bugaj, “Antenna gain measurement by comparative method using an anechoic chamber”, PIERS Proceedings, Moscow, 2012.